Journal of Medicinal Chemistry

Article

pubs.acs.org/jmc

Novel Analgesic/Anti-Inflammatory Agents: 1,5-Diarylpyrrole Nitrooxyalkyl Ethers and Related Compounds as Cyclooxygenase-2 Inhibiting Nitric Oxide Donors

Maurizio Anzini,*[,†] Angela Di Capua,[†] Salvatore Valenti,[†] Simone Brogi,[†] Michele Rovini,[†] Germano Giuliani,[†] Andrea Cappelli,[†] Salvatore Vomero,[†] Luisa Chiasserini,[†] Alessandro Sega,[†] Giovanna Poce,[‡] Gianluca Giorgi,[§] Vincenzo Calderone,[§] Alma Martelli,[§] Lara Testai,[§] Lidia Sautebin,[∥] Antonietta Rossi,[∥] Simona Pace,[∥] Carla Ghelardini,[⊥] Lorenzo Di Cesare Mannelli,[⊥] Veronica Benetti,[#] Antonio Giordani,[∞] Paola Anzellotti,[●] Melania Dovizio,[●] Paola Patrignani,[●] and Mariangela Biava[‡]

[†]Dipartimento Farmaco Chimico Tecnologico, Università degli Studi di Siena, Via A. De Gasperi 2, I-53100 Siena, Italy

[‡]Dipartimento di Studi di Chimica e Tecnologie del Farmaco, Università degli Studi di Roma "La Sapienza", Piazzale Aldo Moro 5, I-00185 Roma, Italy

[§]Dipartimento di Chimica, Università degli Studi di Siena, Via A. De Gasperi 2, I-53100 Siena, Italy

[§]Dipartimento di Psichiatria, Neurobiologia, Farmacologia e Biotecnologie, Università degli Studi di Pisa, Via Bonanno 6, I-56126 Pisa, Italy

[∥]Dipartimento di Farmacia, Università degli Studi di Napoli "Federico II", Via D. Montesano 49, I-80131 Napoli, Italy

[⊥]Dipartimento di Farmacologia, Università degli Studi di Firenze, Viale G. Pieraccini 6, I-50139 Firenze, Italy

[#]Innovative Biotech, Via di Oratoio, 56121 Pisa, Italy

[∞]Rottapharm Madaus, Via Valosa di Sopra 7, I-20052 Monza, Italy

[●]Dipartimento di Neuroscienze ed Imaging, Università degli Studi di Chieti, "G. d'Annunzio" and CeSI, Via dei Vestini 31, I-66100 Chieti, Italy

Supporting Information

ABSTRACT: A series of 3-substituted 1,5-diarylpyrroles bearing a nitrooxyalkyl side chain linked to different spacers were designed. New classes of pyrrole-derived nitrooxyalkyl inverse esters, carbonates, and ethers (**7**−**10**) as COX-2 selective inhibitors and NO donors were synthesized and are herein reported. By taking into account the metabolic conversion of nitrooxyalkyl ethers (**9**, **10**) into corresponding alcohols, derivatives **17** and **18** were also studied. Nitrooxy derivatives showed NO-dependent vasorelaxing properties, while most of the compounds proved to be very potent and selective COX-2 inhibitors in in vitro experimental models. Further in vivo studies on compounds **9a,c** and **17a** highlighted good anti-inflammatory and antinociceptive activities. Compound **9c** was able to inhibit glycosaminoglycan (GAG) release induced by interleukin-1β (IL-1β), showing cartilage protective properties. Finally, molecular modeling and ^{1}H- and ^{13}C-NMR studies performed on compounds **6c**,**d**, **9c**, and **10b** allowed the right conformation of nitrooxyalkyl ester and ether side chain of these molecules within the COX-2 active site to be assessed.

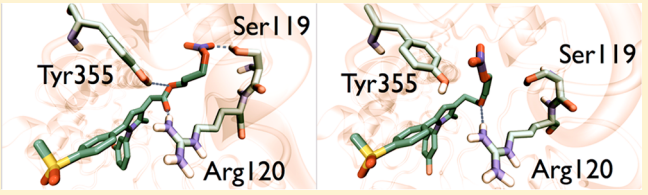

INTRODUCTION

Traditional nonsteroidal anti-inflammatory drugs (tNSAIDs) represent the most widely prescribed, efficacious, and cost-effective pharmacological treatment of rheumatologic and inflammatory disorders.[1] In addition, this class of drugs is widely used to treat mild to moderate pain.[2] Their therapeutic effects are mediated by the inhibition of cyclooxygenase (COX) 2, which is the most important COX isoform contributing to prostanoid generation at inflammatory sites and spinal cord.[3] Selective COX-2 inhibitors (coxibs) have been developed to produce an efficacy comparable to tNSAIDs while reducing gastrointestinal (GI) related adverse events which are mainly due to the inhibition of COX-1-derived cytoprotective prostanoids in the GI tract.[4,5] However, the use of tNSAIDs and coxibs is associated with an increased risk of thrombotic and renal adverse events.[6] This is due to their inhibitory effects on the biosynthesis of vascular prostacyclin (PGI_2), a powerful platelet inhibitor and vasodilator, which is mainly derived from the hemodynamic shear induced by COX-2.[7] Recently, Yu et al.

Received: September 26, 2012
Published: March 27, 2013

showed that vascular COX-2 deletion ends in the reduction of the expression of endothelial nitric oxide (NO) synthase and consequent release of NO.[8] Similar to prostacyclin, NO is endowed with important cardioprotective properties, such as vasodilation and inhibition of platelet function.[9] Suppression of PGI_2 formation due to inhibition of vascular COX-2 is sufficient to account for the cardiovascular (CV) hazard from NSAIDs (traditional and selective for COX-2),[10] but it may be increased by secondary mechanisms such as suppression of NO production.[8]

These findings justify the need to develop NSAIDs endowed with NO-releasing properties in order to mitigate their CV and GI hazard. Indeed, the novel class of anti-inflammatory agents, named COX-inhibiting nitric oxide donors (CINODs), developed by linking a NO-releasing moiety to a tNSAID, has been shown to have a more favorable clinical profile than the parent tNSAIDs in randomized clinical trials.[11,12] This is plausibly due to the property of CINODs to release NO which may replace the functions of inhibited prostanoids by the tNSAIDs.[13]

Naproxcinod, 4-(nitroxy)butyl-(*S*)-2-(6-methoxy-2-naphthyl)propanoate is the first drug of the CINODs, the class of which is in advanced state of development.[14] In randomized clinical trials, naproxcinod showed an improved safety profile with respect to blood pressure (BP) and GI tract compared to naproxen.[15,16] Naproxcinod is the ester of naproxen with 4-(nitroxy)butanol (NOBA) and undergoes hydrolysis, mainly in the GI tract, leading to the release of naproxen and the organic nitrate NOBA. The analgesic and anti-inflammatory activities of naproxcinod are dependent on released naproxen, while NOBA is the main source of NO (for more details, see Supporting Information). A common pathway for NO generation among naproxcinod, NO-flurbiprofen (**3**, a naproxcinod congener, Chart 1), and glyceryl trinitrate (GTN) was recognized.[17,18] NOBA, as well as GTN, is a relatively fast NO-releasing compound, and the CV effects are detected for a maximum of 3 h after the administration with naproxcinod. On the contrary, the analgesic and anti-inflammatory effects of naproxcinod are more extended because they depend on the pharmacokinetics of naproxen which is characterized by a long half-life (i.e., 17 h).[19]

Our research was focused on the development of a new class of coxibs based on the diarylpyrrole scaffold[20−22] and subsequently on the search of NO-releasing compounds endowed with strong analgesic and anti-inflammatory properties. For the sake of completeness, here we report the synthesis and the biological evaluation of a series of 1,5-diarylpyrrole nitrooxyalkyl congeners (**7**−**10**) as a further transformation of the very recently reported nitrooxyalkyl esters (**6**).[23,24] In the title compounds different linkers between the 1,5-diarylpyrrole scaffold and the NO releasing moiety were introduced. Thus, O_2NO-alkyl inverse ester (**7**), carbonate (**8**), and ethers (**9**, **10**) were prepared and evaluated in vitro and in vivo in order to disclose new chemical entities useful in the long term treatment of osteoarthritis (OA) with reduced GI and mainly CV adverse effects (Chart 2). In particular, nitrooxyalkyl ethers **9** and **10** were designed with the aim to prevent the hydrolysis of the side chain, leading to compounds with the inhibitory activity toward COX-2 and NO releasing property in the same molecule. Conversely, with regard to the series of nitrooxyalkyl esters **6**, inhibitory activity toward COX-2 and the NO-releasing property was retained in two different parts of the molecule. These esters, however, showed almost the same liability to esterase previously described for naproxcinod and NO-flurbiprofen.

Chart 1. Structures of Reference Compounds

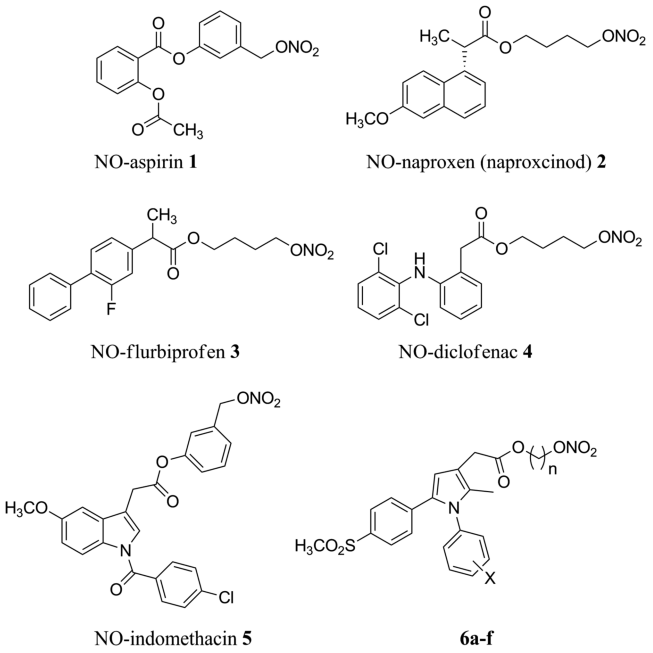

Compd	6a	6b	6c	6d	6e	6f
X	H	H	3-F	3-F	4-F	4-F
n	2	3	2	3	2	3

Chart 2. Structures of 1,5-Diarylpyrrole Nitrooxyalkyl Congeners 7−10

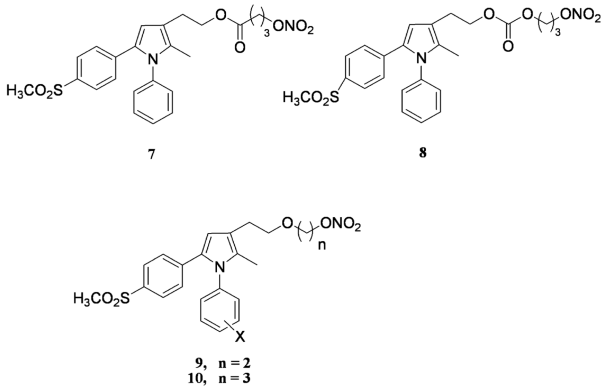

Compd	9a	9b	9c	9d	10a	10b	10c
X	H	3-F	4-F	3,4-F_2	H	3-F	4-F

CHEMISTRY

As is sketched in Scheme 1, hydroxyethyl derivative **11a** was the common starting material for the synthesis of most of the title

dx.doi.org/10.1021/jm301370e | J. Med. Chem. 2013, 56, 3191−3206

Scheme 1. Synthesis of Compounds 7, 8, and 13[a]

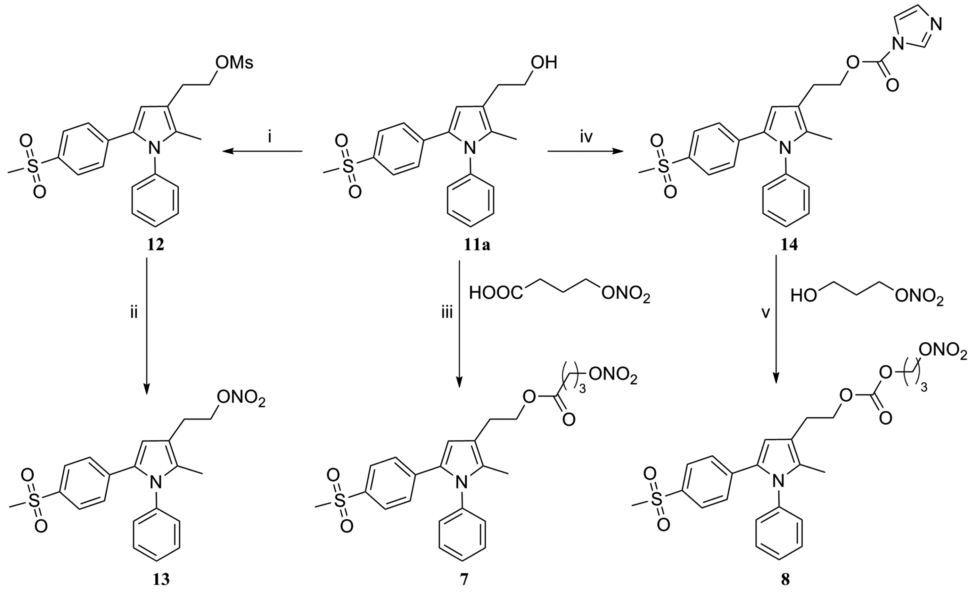

[a]Reagents and conditions: (i) MsCl, DMAP, DIPEA, CH_2Cl_2, 3h, rt; (ii) $(Bu_4N)NO_3$, toluene, reflux; (iii) EDC, DIMAP, CH_2Cl_2, rt, 3 h; (iv) CDI, dry Pyr, rt, 2 h; (v) dry Pyr, DBU, rt, 3 h.

Scheme 2. Synthesis of Compounds 9−11 and 15−20[a]

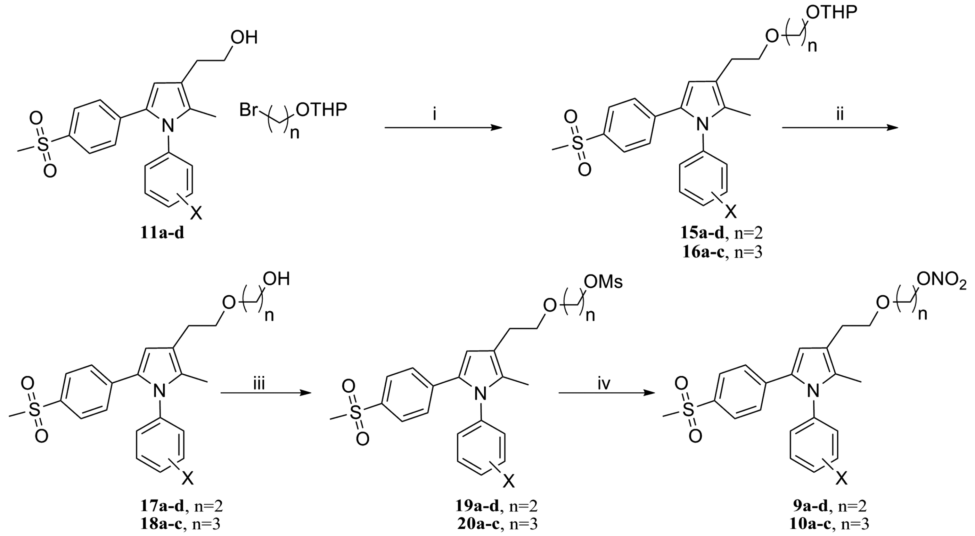

[a]Reagents and conditions: (i) $(Bu_4N)Br$, NaOH 50%, 70 °C, 20 h; (ii) PPTS, MeOH, 55 °C, 20 h; (iii) MsCl, DMAP, DIPEA, rt, 3 h; (iv) $(Bu_4N)NO_3$, toluene, reflux, 1 h.

compounds, and it was prepared in gram scale following the previously-reported procedure.[20,21] The condensation of alcohol **11a** with 4-nitroxybutanoic acid (see Supporting Information) in the presence of EDC and DMAP gave nitrooxyalkyl inverse ester **7**. A different activation of **11a** was requested for the synthesis of compounds **8** and **13**. So compound **11a** was condensed with CDI (1,1′-carbonyldiimidazole) to give imidazocarboxylate **14** which by reaction with hydroxypropan nitrate (see Supporting Information) in dry pyridine and in the presence of 1,8-diazabicyclo[5.4.0]-undec-7-ene (DBU) afforded nitrooxyalkyl carbonate **8**. The transformation of **11a** into the corresponding mesyl chloride **12** and further reaction with $(Bu_4N)NO_3$ in toluene at reflux gave compound **13**. This can be regarded as the simplest among the nitroesters designed. The synthesis of nitrooxyalkyl ethers **9a−d** and **10a−c** (Scheme 2) started with the alkylation of alcohols **11a−d** with the proper hydroxyalkyl bromide in its tetrahydropyranyl protected form (see Supporting Information) to obtain compounds **15a−d** and **16a−c** which were successively deprotected to give hydroxyalkyl ethers **17a−d** and **18a−c**. These ethers were then mesylated to give **19a−d** and **20a−c** and transformed into the expected nitrooxyalkyl ethers **9a−d** and **10a−c** following the same procedure used for the preparation of compound **13**.

RESULTS AND DISCUSSION

An in vitro cell culture (J774 murine macrophage) assay was performed to evaluate the title compounds' inhibitory potency and selectivity on both COX-isoforms. Results showed that in

dx.doi.org/10.1021/jm301370e | J. Med. Chem. 2013, 56, 3191−3206

Table 1. In Vitro COX-1 and COX-2 Inhibitory Activity (J774 Murine Macrophage Assay) of Compounds 6, 9, 10, 17, and 18

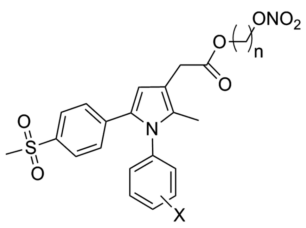

6

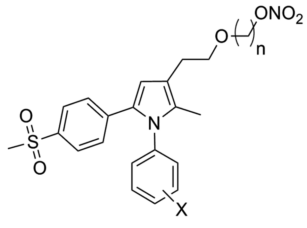

9,10

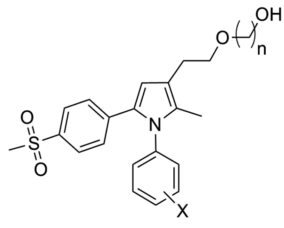

17,18

compd	X	n	IC_{50} (μM)[a] COX-1	IC_{50} (μM)[a] COX-2	COX-1/COX-2 [b]
6a[c]	H	2	>10	0.0430	>232.6
6b[c]	H	3	>10	0.0420	>238.1
6c[c]	3-F	2	>10	0.0190	>526.3
6d[c]	3-F	3	1.1	0.0073	150.7
6e[c]	4-F	2	>10	0.0290	>344.8
6f[c]	4-F	3	>10	0.0372	>268.8
9a	H	2	>10	0.0170	>588.2
9b	3-F	2	>10	0.0270	>357.1
9c	4-F	2	>10	0.0140	>714.3
9d	3,4-F2	2	>10	0.9200	>10.9
10a	H	3	>10	0.0150	>666.7
10b	3-F	3	2.9	0.0230	126.1
10c	4-F	3	>10	0.1900	>52.6
17a	H	2	>10	0.0270	>370.4
17b	3-F	2	>10	0.0460	>217.4
17c	4-F	2	>10	0.0890	>112.3
17d	3,4-F2	2	>10	0.4200	>23.8
18a	H	3	>10	8.9900	>1.11
18b	3-F	3	3.7	0.2400	15.4
18c	4-F	3	>10	0.9400	>10.6

[a]Results are expressed as the mean (n = 3 experiments) of the % inhibition of PGE_2 production by test compounds with respect to control samples. The IC_{50} values were calculated by the GraphPad Instat program. Data fit was obtained by means of the sigmoidal dose−response equation (variable slope) (GraphPad software). [b]In vitro COX-2 selectivity index [IC_{50}(COX-1)/IC_{50}(COX-2)]. [c]See ref 24.

very recently reported 1,5-diarylpyrrole derivatives **6**,[22−24] the transformation of the nitrooxyalkyl ester moiety into a nitrooxyalkyl ether group surprisingly led to very active compounds (**9** and **10**). Some of these were endowed with interesting NO-donating properties along with good and selective COX-2 inhibitory activity ranging from low nanomolar to micromolar values (Table 1). On the basis of the structure−activity relationships (SARs), nitrooxyalkyl ethers **9a−d** and **10a−c** showed, on the whole, a better COX-2 inhibitory activity with respect to the corresponding hydroxyalkyl derivatives **17a−d** and **18a−c**. This result could be due to an electronic interaction of the nitrate group or other interactions of this moiety at the inner hydrophobic channel of the enzyme. On the whole, compounds **9a−d** and **10a−c** appear equipotent to the above-cited nitrooxyalkyl esters **6a−f**. In particular, the inhibitory activity of nitrooxyethyl derivatives **9a−c** seems to be independent of the presence and, to some extent, of the position of the fluorine atom but not of the number of substituents. 3′,4′-Difluoro derivative **9d** is much less active (0.920 μM) than the corresponding unsubstituted or monohalogenated derivative **9a** (0.017 μM) or **9b**,**c** (0.027, 0.014 μM, respectively). A different behavior may be found in nitrooxypropyl ethers **10a−c**. Only nonhalogenated derivative **10a** still retains a potent COX-2 inhibitory activity (0.015 μM). As for 3′- and 4′-fluorinated derivatives **10b** and **10c**, their inhibitory activity has partially decreased. This demonstrates that the presence of the halogen in 4′-position (**10c**) is not fully compatible with the lengthening of the spacer between the O_2NO group and the ethereal oxygen atom of the side chain. This finding was not confirmed when 3′- and 4′-fluorinated nitrooxypropyl esters **6e** and **6f** were taken into account. In fact, both compounds showed a nanomolar COX-2 inhibitory activity, compound **6d** being the most active (0.0073 μM) within the series. In this case, the three-carbon spacer, the presence of the carbonyl group, and the 3′-position of the fluorine atom in the N_1-phenyl ring seem to be the optimal combination for a profitable interaction with the active site of the isoenzyme. Furthermore, among hydroxyethyl- and hydroxypropyl ethers **17a−c** and **18a−c**, which could be regarded as the metabolites of nitroesters **9** and **10**, respectively, compounds **17a−c** showed an efficacious and selective COX-2 inhibitory activity spanning from 0.027 μM for nonhalogenated compound **17a** to 0.046 and 0.089 μM for the 3′-F and 4′-F derivatives, respectively. In this small series of compounds the presence and the position of the fluorine atom, although not appearing to be detrimental to the retaining of the COX-2 inhibitory activity, certainly decrease to some extent the activity of unsubstituted alcohol **17a**. On the contrary, within the series of hydroxylpropyl ethers **18a−c**, the absence of fluorine atom gives rise to the inactive compound **18a**. The presence of the halogen at 3′-position of the N_1-phenyl ring of the pyrrole nucleus in connection with the hydroxylpropyl

dx.doi.org/10.1021/jm301370e | J. Med. Chem. 2013, 56, 3191−3206

chain seems to be decisive for the strong COX-2 inhibitory activity. This inhibitory activity drastically decreases when the fluorine atom is shifted from position 3′ to 4′. As for O_2NO-alkyl inverse ester (**7**) and carbonate (**8**), these compounds were found to be devoid of both activities, being unable to release NO in an efficient way and lacking at the same time the COX-2 inhibitory activity, unlike what happens for compounds **6**, **9**, and **10**. This different behavior may be attributed to the diversity of the functional group inserted as linker between the pyrrole scaffold of compounds **7** and **8** and the nitroester moiety. As a result, its side chains do not seem to have the right stereoelectronic requisites for a profitable interaction with the isoenzyme. Compounds **9a−d** and **10a−c** were further evaluated to assess their efficacy and potency in determining NO-vasorelaxing responses in a suitable experimental model of vascular smooth muscle and, in particular, in endothelium-denuded rat aortic rings. In this experimental approach, five of the seven nitrooxyalkyl derivatives exhibited vasorelaxing effects. In particular, compounds **9a−d** and **10a** evoked a concentration-dependent relaxation of the vascular smooth muscle with potency levels of around 10 μM and efficacy parameters ranging from 43% to 65% (Table 2). Only

Table 2. Evaluation of Efficacy and Potency in Determining NO-Dependent Vasorelaxing Responses of 9a−d, 10a−c, and Gliceryl Trinitrate (GTN)

compd	X	*n*	E_{max} [a]	pIC_{50} [b]
6a[c]	H	2	65 ± 2	5.76 ± 0.08
6b[c]	H	3	44 ± 8	≤5
6c[c]	3-F	2	69 ± 4	6.48 ± 0.06
6d[c]	3-F	3	39 ± 1	≤5
6e[c]	4-F	2	58 ± 5	5.47 ± 0.07
6f[c]	4-F	3	41 ± 2	≤5
9a	H	2	65 ± 3	5.22 ± 0.03
9b	3-F	2	60 ± 4	5.32 ± 0.05
9c	4-F	2	49 ± 4	≤5
9d	3,4-F2	2	43 ± 6	≤5
10a	H	3	48 ± 5	≤5
10b	3-F	3	na	
10c	4-F	3	na	
GTN			93 ± 2	6.90 ± 0.07

[a] E_{max} represents the vasorelaxing efficacy, expressed as a % of the vasoconstriction induced by the preadministration of KCl. [b] The parameter of potency is expressed as pIC_{50}, representing −log of the molar concentration capable of inducing a vasorelaxing effect = 50% of E_{max}. [c] See ref 24.

compounds **10b** and **10c** showed negligible levels of vasorelaxing efficacy (<20%). The experiments carried out in the presence of guanylate cyclase (GC) inhibitor 1*H*-[1,2,4]-oxadiazolo[4,3-*a*]quinoxalin-1-one (ODQ) confirmed that the vasorelaxing effects were due to the release of NO. The effect of ODQ in fact significantly antagonized the vasodilator responses evoked by nitrooxy derivatives **9a−d** and **10a** (Table 2). Previous experiments also showed that corresponding hydroxyalkyl derivatives **17a−d** and **18a−c** were devoid of significant vasorelaxing effects (data not shown). This result further indicated that such a pharmacodynamic feature is due to the nitrooxy group and to its probable biotransformation to NO. Consistent with the data emerged in previous studies,[23,24] the present experimental results indicate some relevant structural aspects capable of influencing the vasorelaxing effects (i.e., the NO-releasing process). In particular, it can be observed again that the length of the alkyl chain bearing the nitrooxy group significantly affects the pharmacological behavior. Indeed, the nitrooxyethyl ethers (two-carbon alkyl chain) exhibit higher levels of vasorelaxing effects than those shown by the corresponding nitrooxypropyl ethers (three-carbon alkyl chain). This is clearly evident from the direct comparison of the couples of analogues **9a** vs **10a**, **9b** vs **10b**, and **9c** vs **10c** (Table 2). It is noted that glyceryl trinitrate (GTN), selected as reference drug endowed with rapid NO-releasing properties, showed strong vasorelaxing effects, with higher levels of vasorelaxing potency (Table 2). Such experimental evidence suggests that the compounds herein reported ensure a NO release slower than GTN, thus acting as a "modulated" NO donor. Thus, we have identified novel hybrid compounds endowed with selective COX-2 inhibitory activity, important for analgesic and anti-inflammatory efficacy, and slow NO-releasing properties that may translate into prolonged protective effects for the cardiovascular system.[25]

On the basis of their very encouraging COX-2 inhibitory activity evidenced in the in vitro tests, compounds **9a−d**, **17a−d**, and **18a** were then selected and submitted to further pharmacological tests to assess their in vivo anti-inflammatory and antinociceptive activities. For this purpose compound effects were evaluated both in a chemical visceral pain model, induced by the intraperitoneal injection of acetic acid (Writhing test), and in the carrageenan-induced inflammatory pain model (Tables 3 and 4). In Table 3 the analgesic effect of compounds **9a−d**, **10a**, **17a−d**, and **18a** compared to that of celecoxib (as reference drug), evaluated as the number of abdominal constrictions induced by intraperitoneal acetic acid, is reported. For each molecule a dose−response curve has been performed. All compounds exhibited an analgesic effect. The minimal dose able to revert the painful condition was 10 mg/kg po for **9a**, **9c**, and **17a**, 20 mg/kg for **9d**, **10a**, **17b**,**d**, **18a**, and 40 mg kg^{-1} for **9b** and **17c**. Celecoxib was able to increase the pain threshold starting from 3 mg/kg.

Moreover, these compounds were assayed in rats to assess their effects on pain threshold alteration and edema induced by carrageenan. Four hours after the intraplantar administration of carrageenan in the paw, all inflammatory signs were observed (paw swelling hyperemia and hyperalgesia). The paw pressure test was used to measure pain. All molecules showed a statistically significant capability to block the painful condition caused by the strong inflammatory agent in the range between 30 and 120 min after administration (Table 4). Thirty minutes after a 20 mg/kg po administration, all compounds showed good activity against carrageenan-induced hyperalgesia. This result was comparable to that obtained with celecoxib (10 mg/kg po). Moreover, with the exception of **9b** and **9d**, for all compounds, at the higher tested dose, the persistence of the antihyperalgesic activity after the injection was longer than 60 min. Compounds **9a**, **9c**, **10a**, **17c**, and **17d** exhibited their efficacy up to 120 min after treatment.

In the carrageenan-induced inflammatory pain model the measure of the paw volume allows discrimination of the analgesic property from the anti-inflammatory one. In Table 4 is shown a significant paw edema decrease 60 min after the administration of all the investigated compounds. These data strongly suggest the anti-inflammatory effect as the base of the analgesic mechanism of these molecules. Finally, the efficacy of compounds **9c** and **17c** was also evaluated in the rat osteoarthritis model induced by the intra-articular injection of

dx.doi.org/10.1021/jm301370e | J. Med. Chem. 2013, 56, 3191−3206

Table 3. Dose–Response Results of Compounds 9a–d, 10a, 17a–d, and 18a in the Acetic Acid Writhing Test[a]

treatment	no. mice	dose per os (mg kg^{-1})	no. writhes
saline	36		32.4 ± 1.9
9a	10	10	21.2 ± 3.0^
9a	8	20	15.5 ± 3.6*
9b	8	10	32.5 ± 3.7
9b	8	20	30.3 ± 2.1
9b	8	40	25.3 ± 3.6*
9c	8	3	28.5 ± 3.2
9c	8	10	19.1 ± 2.7*
9c	8	20	15.2 ± 3.3*
9d	7	10	27.3 ± 2.5
9d	7	20	24.8 ± 3.0*
9d	7	40	25.6 ± 2.3*
10a	9	10	29.4 ± 3.0
10a	10	20	21.2 ± 3.0*
10a	8	40	26.8 ± 3.2^
17a	8	10	21.2 ± 3.0*
17a	8	20	15.5 ± 3.6*
17b	8	10	29.4 ± 3.0
17b	8	20	26.8 ± 3.2^
17b	8	40	17.3 ± 3.5*
17c	7	10	31.3 ± 2.7
17c	8	20	27.9 ± 3.6
17c	8	40	18.2 ± 3.1*
17d	9	10	32.3 ± 2.8
17d	8	20	26.3 ± 3.4^
17d	8	40	17.3 ± 2.2*
18a	9	10	29.7 ± 3.4
18a	9	20	22.3 ± 2.5*
18a	7	40	21.5 ± 2.3*
celecoxib	10	1	25.6 ± 3.1*
celecoxib	11	3	15.4 ± 2.5*
celecoxib	15	10	11.3 ± 2.9*

[a]Each value represents the mean of at least seven mice: (^) $P < 0.05$, (*) $P < 0.01$ in comparison with CMC treated group.

monoiodoacetate (MIA). The injection of MIA in the knee joint induces necrosis of condrocytes with decrease of cartilage thickness and osteolysis.[26] Kobayashi et al. showed that MIA is able to disorganize condrocytes and to promote cartilage erosion.[27] These alterations are comparable with joint damages typical of humans affected by osteoarthritis.[28−30] An amount of 20 mg kg^{-1} compound **9c** or **17c** was administered po twice daily for 13 days starting from the day of MIA injection to evaluate a preventive effect. On day 14, when pain and the degenerative articular process are overt, the pain threshold was measured by paw pressure test (Table 5). The repeated treatment with **9c** or **17c** significantly prevented MIA-dependent hyperalgesia (before treatment). A further compound administration (after treatment, 30 min) did not induce an additive acute antihyperalgesic effect, suggesting that a repeated treatment with the present anti-inflammatory compounds could be able to prevent the joint damage and, consequently, pain.[28−31]

Study of cartilage catabolism in culture has received considerable attention over the past 3 decades because of the pivotal role that this process plays in cartilage degeneration in arthritis.[32] From realization that such degeneration is driven by cytokines, cartilage organ culture became a standard technique for monitoring the effects of cytokines on chondrocytes metabolism. Under such conditions proteoglycans degradation was found to be an early event, with the glycosaminoglycans (GAG) rich degradation products being readily released from the tissue into the culture medium.[33] Therefore, following the assessment of their anti-inflammatory and antinociceptive activity, nitrooxyethyl ether derivative **9c** and its metabolite **17c** were selected and tested to determine their cartilage protective properties. The test consisted of quantitation of GAG in the form of aggrecan fragments released from bovine articular cartilage of the metacarpophalangeal joints of the feet. After being cultured according to the procedure reported by Homandberg et al.[34] (see Supporting Information), fragments were challenged for 48 h with IL-1β (30 ng/mL) and quantitation of GAG release was assessed by means of most widely used Farndale's colorimetric method.[35] Results are shown in Figure 1. Compounds **9c** and **17c** were able to inhibit GAG release induced by IL-1β in a concentration-dependent manner (IC_{50} of 1.5 and 33 μM, respectively). Treatment with **9c**, **17c**, or IL-1β did not affect the viability of cell recovery from cartilage. Our results show that compound **9c** can contribute to the reduction of IL-1β-dependent cartilage catabolism both by the inhibition of prostanoid biosynthesis and by NO releasing properties. Neverthless, the release of NO by **9c** seems to play a major role. This assumption is based on the fact that compound **17c**, which was unable to release NO, was found to be 22-fold less potent than the parent compound, although its activity in inhibiting COX-2 activity in murine J774 cells was comparable to that of **9c**.

With the aim of assessing COX-2 selectivity, a human whole blood (HWB) assay was carried out on selected compounds **9c** and **17c** (nitrooxy ether and hydroxyethyl ether, respectively). In particular, the assay was performed to predict the actual extent of isozyme inhibition achievable in vivo by circulating drug levels to consider the amount of variables potentially able to affect drug–enzyme interaction. As shown in Figure 2 (panels A and B) the concentration–response curves for inhibition of COX-1 and COX-2 in human whole blood elicited by **9c** and **17c**, respectively, were studied. Nitrooxy ether derivative **9c** and its NO-free metabolite **17c** inhibited LPS-induced whole blood PGE_2 generation (COX-2 assay) in a concentration-dependent fashion with IC_{50} values (Table 6) significantly comparable. The steepness of the curves by calculating the Hill slope values was also studied. The **9c** Hill slope value was significantly comparable to 1.0, which is typical for a standard sigmoid concentration–response curve where response (Y) is a function of the logarithm of compound concentration (X). The Hill slope value of **17c** was slightly, but significantly, less than 1.0 (Table 6). As has been previously reported,[36] NSAIDs that inhibit COX activity with a Hill slope value of 1.0 are freely reversible and exhibit simple competitive inhibition. Since the administration of an analgesic dose of NSAIDs is associated with a 80% inhibition of whole blood COX-2 activity,[37] the IC_{80} values for these compounds were calculated. As shown in Table 6, compounds **9c** and **17c** showed comparable IC_{80} values in inhibiting COX-2. Taken together, these results suggest that nitrooxyethyl ether derivative **9c** and its metabolite **17c** have a comparable and potent inhibitory effect on monocyte COX-2 activity of HWB. Furthermore, **9c** and **17c** inhibited platelet COX-1 activity in a concentration-dependent fashion (Figure 2, panels A and B); however, **17c** was slightly, but significantly, more potent in the inhibition of COX-1 rather than **9c** (both at IC_{50} and IC_{80}) (Table 6). Interestingly, both compounds inhibited COX-1

Table 4. Effect of Compounds 9a–d, 10a, 17a–d, and 18a on Hyperalgesia and Edema Induced by Carrageenan in the Rat Paw Pressure Test[a]

		paw pressure in rats (g)					
			after treatment			paw volume (mL)	
pretreatment intraplantar	treatment per os	before treatment	30 min	60 min	120 min	before treatment	60 min
saline	saline	62.6 ± 2.4	61.5 ± 3.1	60.2 ± 3.3	62.9 ± 3.5	1.46 ± 0.05	1.42 ± 0.07
carrag	saline	31.4 ± 3.4	34.8 ± 3.0	33.9 ± 3.7	31.4 ± 3.7	1.47 ± 0.07	2.48 ± 0.06
carrag	**9a** 20	33.9 ± 3.1	54.2 ± 3.1*	55.3 ± 3.5*	48.7 ± 3.7^	1.31 ± 0.09	1.45 ± 0.10*
carrag	**9b** 20	34.6 ± 3.0	43.9 ± 3.1^	40.7 ± 3.0	35.2 ± 3.5	1.58 ± 0.08	2.16 ± 0.09^
carrag	**9b** 40	31.6 ± 2.7	47.3 ± 4.2*	41.0 ± 4.4	34.3 ± 4.1	1.55 ± 0.09	2.08 ± 0.07*
carrag	**9c** 10	34.1 ± 2.7	55.1 ± 4.7*	52.6 ± 4.0*	48.3 ± 5.2^	1.49 ± 0.08	1.87 ± 0.07*
carrag	**9c** 20	32.0 ± 3.5	56.8 ± 3.9*	49.2 ± 4.6*	43.8 ± 4.5^	1.53 ± 0.08	1.92 ± 0.08*
carrag	**9d** 20	32.7 ± 3.7	44.6 ± 4.0^	46.9 ± 4.2^	38.8 ± 3.5	1.54 ± 0.06	2.19 ± 0.07^
carrag	**9d** 40	35.2 ± 3.1	49.5 ± 3.8*	42.5 ± 4.1	35.3 ± 3.8	1.48 ± 0.07	2.10 ± 0.08*
carrag	**10a** 20	32.9 ± 3.3	53.7 ± 3.4*	51.6 ± 3.2*	45.6 ± 3.4^	1.53 ± 0.06	1.80 ± 0.04*
carrag	**17a** 20	31.8 ± 3.2	56.6 ± 4.3*	49.2 ± 3.8^	37.8 ± 3.6	1.26 ± 0.05	1.34 ± 0.07*
carrag	**17b** 20	32.7 ± 3.9	46.9 ± 3.8^	48.6 ± 3.5^	37.2 ± 3.9	1.55 ± 0.08	2.46 ± 0.08
carrag	**17b** 40	33.5 ± 3.9	51.4 ± 3.0*	45.3 ± 4.4^	39.5 ± 4.0	1.49 ± 0.09	2.12 ± 0.06^
carrag	**17c** 20	32.5 ± 3.4	46.8 ± 3.7*	38.7 ± 3.3	38.3 ± 3.9	1.57 ± 0.07	2.01 ± 0.09*
carrag	**17c** 40	30.5 ± 3.5	57.2 ± 4.6*	58.3 ± 4.5*	47.6 ± 4.4^	1.55 ± 0.09	1.95 ± 0.08*
carrag	**17d** 20	31.6 ± 2.8	43.6 ± 3.8^	46.7 ± 3.5^	41.4 ± 4.7	1.56 ± 0.08	2.16 ± 0.08^
carrag	**17d** 40	34.1 ± 3.3	53.2 ± 3.4*	55.2 ± 4.2*	49.3 ± 3.6*	1.58 ± 0.09	1.96 ± 0.06*
carrag	**18a** 20	33.8 ± 3.8	52.9 ± 3.6*	50.3 ± 2.9*	46.6 ± 3.1^	1.47 ± 0.05	1.86 ± 0.04*
carrag	celecoxib 3	31.7 ± 2.7	44.3 ± 3.8*	41.6 ± 3.2	40.7 ± 2.6	1.59 ± 0.08	2.35 ± 0.07
carrag	celecoxib 10	33.5 ± 2.6	52.9 ± 3.1*	48.3 ± 3.4*	39.8 ± 3.1	1.50 ± 0.05	1.45 ± 0.06*

[a]There were four rats per group: (∧) $P < 0.05$, (∗) $P < 0.01$ versus the carrageenan/saline-treated group; carrag = carrageenan.

Table 5. Effect of Repeated Treatment with Compounds 9c and 17c on Hyperalgesia Induced by Osteoarthritis in the Paw Pressure Test[a]

		paw pressure in rats (g)	
pretreatment, intra-articular	treatment, per os	before treatment	after treatment (30 min)
saline	CMC	61.2 ± 3.0	58.7 ± 2.9
MIA[b]	CMC	32.6 ± 2.9	30.4 ± 3.1
MIA[b]	**9c** (20)	43.5 ± 2.9*	45.1 ± 3.7*
MIA[b]	**17c** (20)	49.7 ± 3.5*	51.2 ± 3.9*

[a]There were four rats per group: (∗) $P < 0.01$ versus the MIA treated rat. [b]MIA = monosodium iodoacetate.

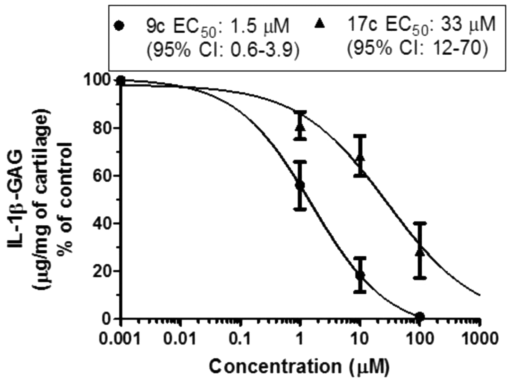

Figure 1. Effect of compounds **9c** and **17c** on glycosaminoglycans (GAG) released from bovine articular cartilage challenged for 48h with IL-1β (30 ng/mL). Results are expressed as percent of control (IL-1β alone) (mean ± SEM, $n = 3$). EC_{50} (**9c** and **17c** concentration that is reduced by 50% IL-1β-induced GAG release) and its 95% confidence intervals (CI) are shown.

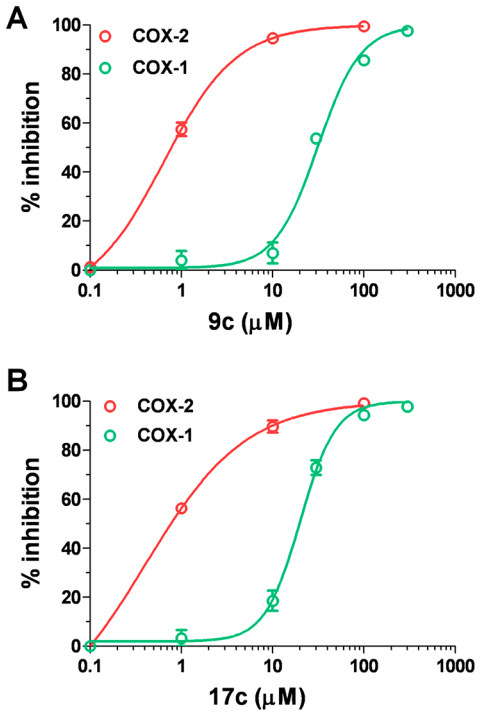

Figure 2. Effects of compounds **9c** and **17c** on in vitro platelet COX-1 and monocyte COX-2 activity in human whole blood. Results are expressed as average percentage of inhibition (N = 3–6, mean ± SEM).

activity with Hill slope values of >1.0 (Table 6), normally a feature of steeper curves. A time-dependent COX inhibiting effect was observed by NSAIDs with Hill slope values of >1.0.[36] Selectivity of **9c** and **17c** toward COX-2 was determined as IC_{50} and IC_{80} ratios for the inhibition of whole blood COX-1

dx.doi.org/10.1021/jm301370e | J. Med. Chem. 2013, 56, 3191–3206

Table 6. IC_{50} and IC_{80} Values, Hill Slopes, and COX-2 Selectivity of Compounds 9c and 17c in Human Whole Blood (HWB) Assays[a]

	9c		17c	
	COX-2	COX-1	COX-2	COX-1
IC_{50} (μM)	0.64 (0.43−0.96)	31.24 (26.16−36.55)	0.40 (0.19−0.83)	20.00 (17.33−23.10)
Hill slope	1.10 (0.73−1.46)	1.85 (1.37−2.33)	0.79 (0.59−0.98)	2.24 (1.72−2.77)
IC_{50}(COX-1)/IC_{50}(COX-2) [b]	50.00		50.00	
IC_{80} (μM)	2.26	63.3	2.31	37.14
IC_{80}(COX-1)/IC_{80}(COX-2) [b]	29.33		16.07	

[a]For IC_{50} values and Hill slopes, 95% confidence intervals are shown in parentheses. [b]Selectivities of compounds toward COX-2 were determined as IC_{50} and IC_{80} ratios for HWBA-COX-1 and COX-2.

and COX-2. As shown in Table 6, both compounds were 50-fold more potent toward COX-2 than COX-1 at IC_{50}. A lower COX-2 selectivity was found at IC_{80}.

In conclusion, **9c** and its metabolite **17c** are potent and selective inhibitors of COX-2. Although further studies should be performed, our data may suggest that **9c** and **17c** inhibited COX-2, but not COX-1, in a time-dependent fashion.

Altogether our results offer proof-of-concept that compounds endowed with dual pharmacological activities, i.e., selective COX-2 inhibition and NO-releasing properties, show analgesic and anti-inflammatory effects in experimental rodent models in vivo. Our results indicate that COX-2 inhibition is the central mechanism for obtaining analgesic and anti-inflammatory effects. Similarly, in randomized clinical trials naproxcinod has been shown to cause comparable relief of the signs and symptoms of OA.[38] However, we showed in vitro that the NO-releasing properties of novel compound **9c** introduced an additional protective effect by preventing cartilage matrix degradation compared to compound **17c** which was unable to release NO. Indeed, NO, at low concentrations, has been previously reported to play protective roles in the joint.[39]

Molecular Modeling Simulations. To better understand the inhibitor−enzyme interactions and to improve our previously proposed mode of binding of NO donors and COX-2 inhibitors **6**,[24] compounds **6d** and **10b** were submitted to rigorous ab initio calculations along with molecular docking and molecular dynamics simulations. In particular, compounds **6d** and **10b** were built starting from the X-ray crystallographic data of **6c** (Figure S1 in the Supporting Information) and then optimized by means of the ab initio restricted Hartree−Fock (RHF) method[40] taking into account the generic nuclear Overhauser effect (NOE) constraints[41] resulting from ^{1}H-NMR solution studies (see Supporting Information). The partial atomic point charges of compounds **6d** and **10b** were calculated by the RHF method[40] and used in the following molecular docking calculations. The binary complexes of compounds **6d** and **10b** with isozyme COX-2 (PDB entry 6cox), obtained from flexible docking simulations and performed by means of Autodock 4.2,[42] were subjected to an extensive molecular dynamics study aimed at investigating (i) the binding mode profile of new derivatives, (ii) the stability of the previously published binding mode[24] of nitrooxyalkyl esters **6c** and **6d**, and (iii) the main intermolecular interactions based on a large time-scale simulation. During 5 ns of molecular dynamics simulations, the complexes showed a geometric stable profile according to which the binding mode of compound **6d** did not substantially diverge from the one previously reported,[24] confirming the significance of the docking results obtained on that occasion. This is the reason why in the present study only the main interactions between the lateral side chain bearing the -ONO_2 moiety of the 1,5-diarypyrrole derivatives **6d** and **10b** and the COX-2 active site were taken into account and discussed. During the whole molecular dynamics, compound **6d** by means of the two oxygen atoms of the carboxypropyl group can engage, permanently, a double hydrogen bond interaction with ARG 120 and TYR 355. Thus, the nitroester group is allowed to lie near SER 119, favoring in this way an additional hydrogen bond interaction of one of the oxygen atoms with the hydroxyl group of such an amino acid (Figure 3).

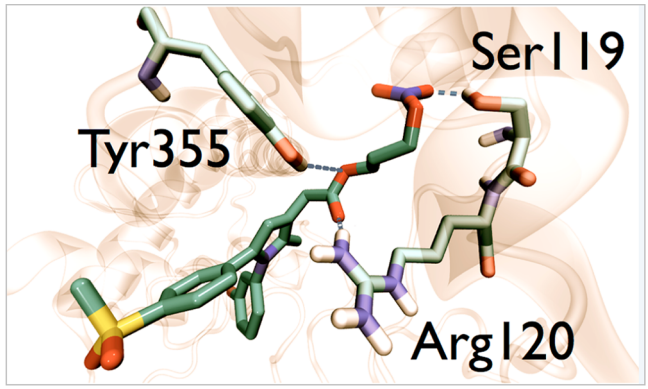

Figure 3. Snapshot of the molecular dynamics simulation of nitrooxypropyl ester **6d** into the COX-2 active site. The main residues and the inhibitor are represented as licorice. Hydrogen bonds are represented as blue dotted lines. For the sake of clarity, only the lateral side chain interacting residues are displayed.

When a 5 ns trajectory from a molecular dynamics simulation (MD) of the complex of nitrooxypropyl ether **10b** with the active site of COX-2 is analyzed, the hydrogen bond interaction between one of the oxygen atoms of the nitro group and SER 119 is completely lost in favor of a different orientation of the lateral side chain which seems to be no more extended than it appears in compound **6d** (Figure 5). In addition, the hydrogen bond between ARG 120 and the ethereal oxygen of compound **10b** is not permanently present during the MD simulation (Figure 4).

On the whole, according to the molecular dynamics simulations, it appears that the conformation of the lateral side chain of the inhibitors along with the hydrogen bond interaction with the SER 119 has to be considered responsible for the different COX-2 inhibitory activities of compounds **6d** and **10b**, the IC_{50} being 7.3 and 23.0 nM, respectively. On the other hand, compound **9d** shows a different binding mode with respect to compounds **6d** and **10b**. In particular, compound **9d** is not able to form any hydrogen bond with SER 119 and the

dx.doi.org/10.1021/jm301370e | J. Med. Chem. 2013, 56, 3191−3206

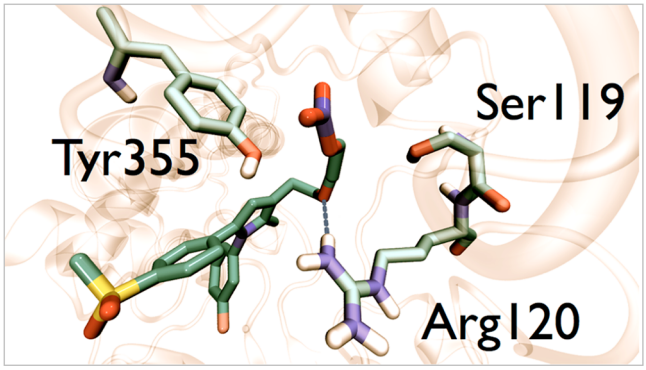

Figure 4. Snapshot of the molecular dynamics simulation of nitrooxypropyl ether **10b** into the COX-2 cyclooxygenase site. The main residues and the inhibitor are represented as licorice. Hydrogen bonds are represented as blue dotted lines. For the sake of clarity, only the lateral side chain interacting residues are displayed.

polar contact to the ARG 120 is actually infrequent during the molecular dynamics simulation studies. These differences, in agreement with the biological data, are probably due to the stereoelectronic effects induced by the introduction of 3′,4′-difluoro substituents coupled to a short lateral side chain linker.

^{1}H- and ^{13}C-NMR Studies Performed on Compounds 6c,d, 9c, and 10b. NMR analysis has been done with the aim of determining both dynamics and conformations of compounds **6c,d**, **9c**, and **10b** the atoms of which have been numbered according to Figure 5. It is known that ^{13}C R_1 ($R_1 = 1/T_1$) relaxation rates are almost exclusively determined by dipolar interactions with directly bonded or nearby protons, thus allowing suitable delineations of the molecular dynamics.[43,44] The motional features of aromatic carbons were considered first, since they have fewer degrees of freedom than side chain carbons. For ring B of compounds **6c**, **6d**, and **10b**, the relaxation rate of C_{14} was faster than those of the other carbon atoms, suggesting that C_{11}−C_{14} is the main rotation axis for this aromatic ring. The relaxation rates of C_{12}, C_{15}, and C_{16} were very similar so that an anisotropic model consisting of rotational reorientation around the main rotation axis with some degree of internal motion could be applied[45] (eq 1 with $A = 0.25(3\cos^2\alpha - 1)^2$, $B = 3(\sin^2\alpha\cos^2\alpha)$, and $C = 0.75(\sin^4\alpha)$).

$$\frac{1}{nT_1} = \frac{\hbar^2\gamma_H{}^2\gamma_C{}^2}{r_{CH}{}^6}\tau_{C,B}\left\{A + B\frac{3\tau_{g,B}}{3\tau_{g,B} + \tau_{C,B}} + C\frac{6\tau_{g,B}}{6\tau_{g,B} + \tau_{C,B}}\right\} \quad (1)$$

In eq 1, $\tau_{c,B}$ is the main rotation correlation time, $\tau_{g,B}$ is the correlation time for librational motions of aromatic ring B, r_{CH} is the length of the C−H bond, n is the number of protons attached to the carbon under consideration, and γ is the angle between the main rotation axis and the C−H vector. The main correlation time, $\tau_{c,B}$, can be calculated by considering the relaxation rate R_1 ($=1/T_1$) of C_{14}. Since the C_{14}−H_{14} vector lies on the main axis, eq 2 can be applied.

$$\frac{1}{nT_1} = \frac{\hbar^2\gamma_H{}^2\gamma_C{}^2}{r_{CH}{}^6}\tau_C \quad (2)$$

This holds for a pure dipole−dipole relaxation mechanism within the extremely narrow region.[46] As all protonated carbons exhibit maximum ^{13}C−^{1}H nuclear Overhauser effects, eq 2 was used to extract $\tau_{c,B}$. $\tau_{g,B}$ was then obtained by applying eq 1. The same analysis holds for ring A: the relaxation rates of C_7 and C_8 are very similar and the main rotation axis is C_6−C_9, as is expected for a para-disubstituted benzene.

Thus, the same anisotropic model can be applied. However, it is impossible to calculate $\tau_{c,A}$, the main correlation time of ring A, from the relaxation rates of carbon atoms. Proton relaxation rates must be used. Indeed, the H_7−H_8 vector is parallel to the main axis C_6−C_9, and by taking advantage of double selective and selective relaxation rates, eq 3 can be written (see Supporting Information):

$$R_{7,8}{}^7 - R_S{}^7 = \sigma_{7,8} = \frac{1}{2}\frac{\hbar^2\gamma_H{}^4}{r_{7,8}{}^6}\tau_{C,A} \quad (3)$$

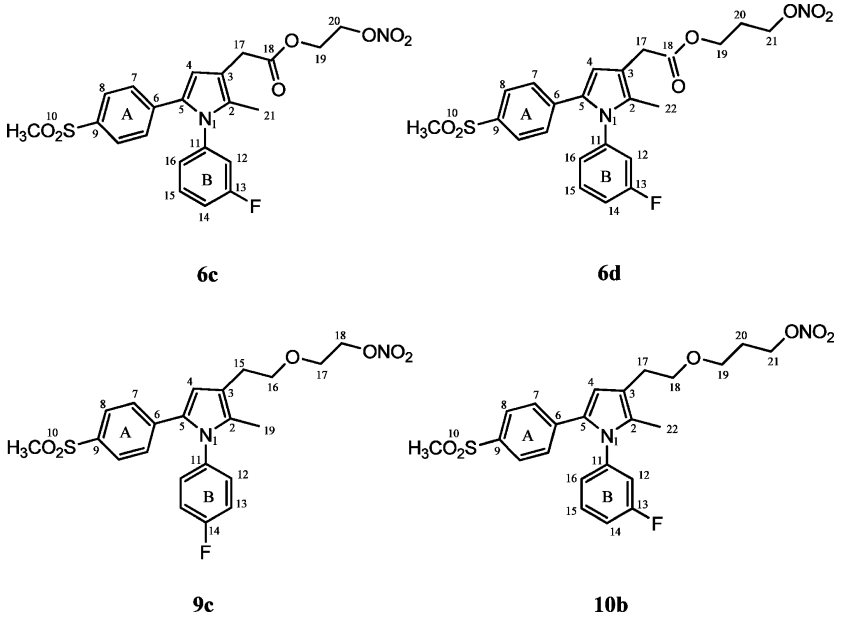

Figure 5. Numbering of atoms of compounds selected for ^{1}H- and ^{13}C-NMR studies.

dx.doi.org/10.1021/jm301370e | J. Med. Chem. 2013, 56, 3191−3206

Table 7. Correlation Times τ_c and τ_g (s) of Compounds 6c,d, 9c, and 10b

parameter	6c	6d	9c	10b
		Aromatic Rings		
τ_c (A)	0.68×10^{-12}	0.84×10^{-12}	0.76×10^{-12}	0.68×10^{-12}
τ_g (A)	0.38×10^{-12}	0.19×10^{-12}	0.48×10^{-12}	0.25×10^{-12}
τ_c (B)	0.63×10^{-12}	0.84×10^{-12}		1.10×10^{-12}
τ_g (B)	0.48×10^{-12}	0.32×10^{-12}		0.39×10^{-12}
τ_c (C-4)	0.64×10^{-12}	0.70×10^{-12}	0.67×10^{-12}	0.79×10^{-12}
		Methylene Groups		
τ_c (C-15)			0.31×10^{-12}	
τ_c(C-16)			0.24×10^{-12}	
τ_c (C-17)	0.34×10^{-12}	0.41×10^{-12}	0.18×10^{-12}	0.46×10^{-12}
τ_c (C-18)			0.22×10^{-12}	0.38×10^{-12}
τ_c (C-19)	0.14×10^{-12}	0.18×10^{-12}		0.24×10^{-12}
τ_c (C-20)	0.18×10^{-12}	0.20×10^{-12}		0.23×10^{-12}
τ_c (C-21)		0.14×10^{-12}		0.16×10^{-12}
		Methyl Groups		
τ_c (C-10)	0.12×10^{-12}	0.14×10^{-12}	0.16×10^{-12}	0.19×10^{-12}
τ_c (C-19)			0.08×10^{-12}	
τ_c (C-21)	0.05×10^{-12}			
τ_c (C-22)		0.07×10^{-12}		0.05×10^{-12}

where $r_{7,8}$ is the H_7–H_8 interproton distance (it has been determined from neutron scattering data that $r_{7,8}$ = 2.45 Å).[47] Then from eq 3 the $\tau_{c,A}$ is obtained and by applying eq 1 again, the corresponding correlation times for librational motions ($\tau_{g,A}$) were calculated. This last approach should also have been applied to ring B of compound **9c** (in this compound both benzene rings are para-disubstituted). However, the proton resonances of H_{12} and H_{13} overlap and it was impossible to evaluate the corresponding relevant proton relaxation rates. The correlation times of the side chain carbons and of C-4 (pyrrole ring) were evaluated from eq 2 (see Table 7).

The analysis of the data show that the main correlation times within each compound are similar or very similar to each other and to the correlation time of C-4 (pyrrole ring). Thus, this result suggested that the motions within the aromatic moieties of these compounds are correlated, and consequently a mean main conformation is present. As expected, the motional freedom increases (τ_c values decreases) along the side chains. However, the compounds with the shorter ethyl side chain (**6c** and **9c**) have greater conformational freedom than the corresponding compounds with propyl side chains (**6d** and **10b**). The conformational analysis has been performed by exploiting qualitative analysis of 1D NOE (difference experiments; for further details see Supporting Information) and 2D NOE (NOESY) experiments.[48,49] The NOE experiments have been performed in 0.1 and 0.01 M solutions. Since the results are very similar, it can be safely assumed that the NOE effect is intramolecular. Moreover, the distance between H_4 and H_7 protons in all compounds could be evaluated by quantitative 1D NOE data analysis[50] (Table 8). This distance $r_{4,7}$ ranges from 2.5 Å (**9c**) to 2.6 Å (**6d** and **10b**) and 2.7 Å (**6c**). The same distances have been determined by analysis of proton relaxation rates (see Supporting Information), and as is shown in Table 8, their values are very close to the corresponding values determined by 1D NOE experiments.

In addition to these distances, $r_{4,7}$ have values that are close to each other in the whole series of compounds. Also, NOE effects have been found between the protons of the methyl bonded to the C_2 of pyrrole ring and the protons of ring B: H_{12} (**9c**) or H_{12} and H_{16} (**6c**, **6d**, and **10b**). These results confirmed

Table 8. Proton–Proton Distances r (Å) in Compounds 6c,d, 9c, and 10b Estimated from Relaxation Rates (a) and $^1H\{^1H\}$NOEs (b) (0.1 M) and Corresponding Dihedral Angles θ (deg) between Ring A and Pyrrole Ring

	6c		6d		9c		10b	
parameter	a	b	a	b	a	b	a	b
$r_{4,7}$	2.5_5	2.7	2.6	2.6	2.4_5	2.5	2.5	2.6
θ	35	44	38	38	33	36	32	38

the evidence of aromatic moieties with restricted internal motions with a preferred mean main conformation that is practically the same in all these molecules. Thus, the core of these molecules is characterized by almost the same dynamical and conformational features independent of different side chains. The analysis of NOE data also allowed the delineation of important conformational details of the side chains. We first consider the compounds with the ester function in their side chain (**6c** and **6d**). In both these compounds there is a NOE effect between H_4 and the first methylene group (H_{17}) of the side chain. In **6c** there are no NOE effects between H_{19} and H_{20} methylene protons and other protons of the molecule; the chain folds away from the aromatic moiety and H_{17}. In **6d** NOE effects have been found between H_{19} and H_{20} methylene protons and the protons (H_{22}) of the methyl group bonded to C_2. This chain presents a partial folding toward the methyl group. The NOE analysis also showed significant differences in the mean main conformations of the two compounds with the ether function in their side chain (**9c** and **10b**). An unexpected NOE effect was found for compound **9c**. It involved side chain protons H_{16} and H_{17}. The chain simply moves straight away from the aromatic moiety. In **10b** there are NOE effects between the protons of the first two methylene groups (H_{17} and H_{18}) and H_4 while the protons of the propyl moiety show no NOE effects with other protons of the molecule. The chain presents an initial folding toward H_4 and then moves straight away. Further insight into the conformations of the side chains was obtained by considering the coupling system of their protons (see Supporting Information, in particular Table S1 and Figure S4). In compounds **9c** and **10b** the protons of the

dx.doi.org/10.1021/jm301370e | J. Med. Chem. 2013, 56, 3191–3206

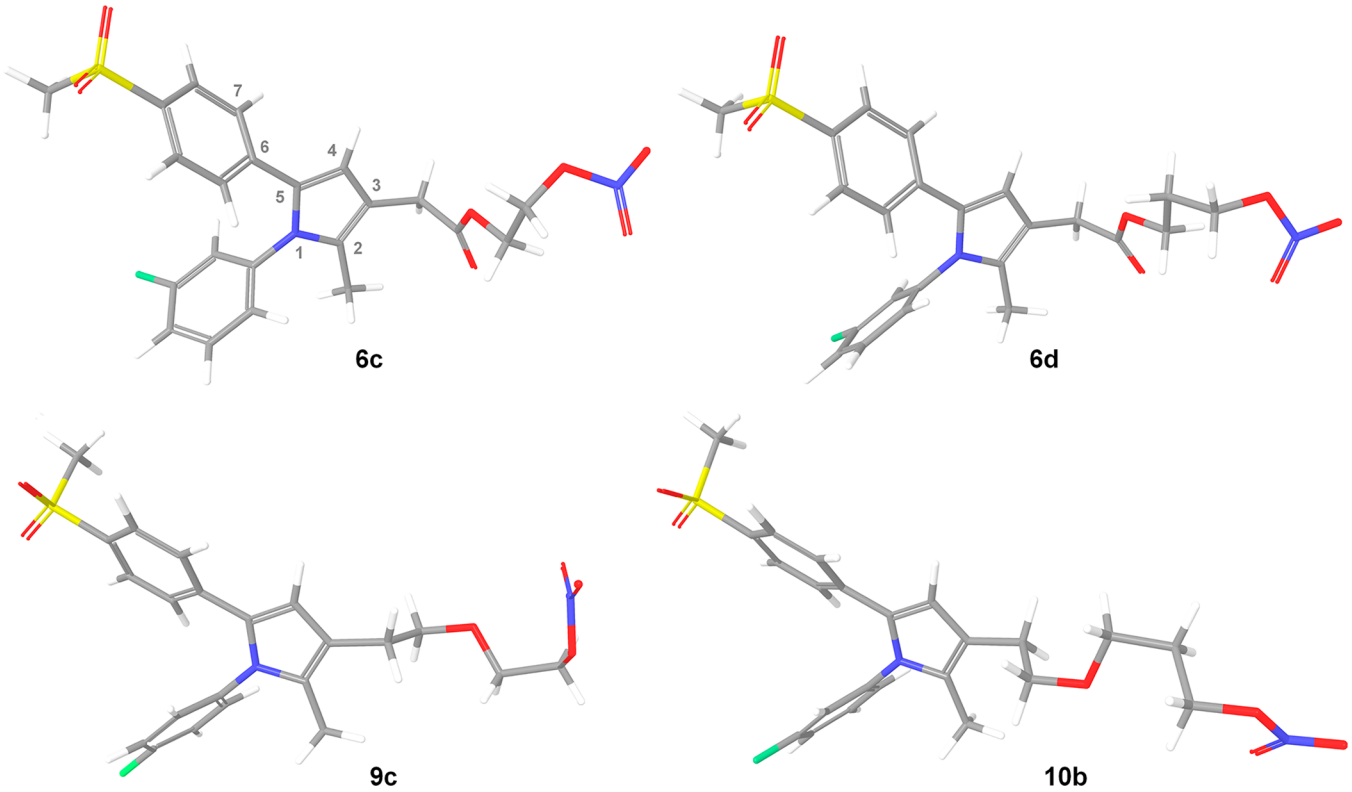

Figure 6. Optimized structure of the compounds used in NMR studies performed by means of NWChem (100 steps of RHF, 6-31G*) using $CHCl_3$ as the solvent, mimicking the experimental conditions in which the spectra were recorded and taking into account the NOE constraints resulting from NMR solutions.

first two methylene groups give rise to two triplets as expected for protons of alkyl chains that adopt the usual all-trans conformations. The same situation is presented by the protons of the propyl chain of compounds **6d** and **10b** (H_{19}, H_{20}, and H_{21}), two triplets (H_{19} and H_{21}) and a quintet (H_{20}) corresponding once again to the all-trans conformation. The situation is completely different for the ethyl moieties of compounds **6c** (H_{19} and H_{20}) and **9c** (H_{17} and H_{18}). These protons give complex multiplets, and this means that the protons within each methylene group are not equivalent. This in turn means that the conformations are gauche conformations around the bonds $C_{19}-C_{20}$ (**6c**) and $C_{17}-C_{18}$ (**9c**). In conclusion, these molecules have an aromatic moiety that does not differ in dynamics and conformation from one compound to the other while the side chains stemming out of the aromatic core have their own dynamics and very different conformations (they explore different conformational spaces). This different behavior of the side chains is likely to be responsible for the fine-tuning and consequently different response in their interactions with the receptor.

A representation of the mean main conformations of compounds **6c**,**d**, **9c**, and **10b**, as was deduced from NMR analysis, is shown in Figure 6.

CONCLUSION

The combination of a COX-2 inhibitor with an appropriate NO-donor moiety can be the bases for the development of new drugs endowed with strong analgesic and anti-inflammatory properties. With no adverse effects on the GI and with an appropriate CV and renal safety, they might be used in long-term treatments and in the elderly population. Obtaining a drug acting as both COX-2 inhibitor and NO donor without being hydrolyzed was pursued in this work in order to provide new drugs endowed with the same pharmacokinetic properties for both the COX inhibitor and the NO-donor moieties which could provide COX-2 inhibition and NO suitable concentrations at the same time and in the same compartment. In addition, particular attention to NO-releasing properties of the obtained compounds was given in order to improve CV-protective properties and to take advantage of the above-discussed favorable effects exerted by low NO concentrations on inflammatory and cartilage degradation processes. In particular, five of the seven nitrooxyalkyl derivatives exhibited vasorelaxing effects. Among them, nitrooxyethyl ethers (two-carbon alkyl chain), **9a**−**c**, show vasorelaxing effect higher than that shown by the corresponding nitrooxypropyl ethers (three-carbon alkyl chain). By taking into account the metabolic conversion of nitrooxyalkyl ethers (**9** and **10**) into corresponding alcohols, derivatives **17** and **18** were also studied. Most of the compounds were found to be very potent and selective COX-2 inhibitors. Compounds **9a**,**c** and **17a**,**c** were selected for further in vivo studies that highlighted good anti-inflammatory and antinociceptive activities. From tests on bovine articular cartilage, **9c** showed cartilage protective properties owing to the inhibition of GAG release induced by IL-1β in a concentration-dependent manner. Finally, compounds **9c** and **17c**, tested on human whole blood (HWB), were found to be selective inhibitors of COX-2. Full ab initio calculations along with molecular docking, molecular dynamics simulations, and ^{1}H- and ^{13}C-NMR studies, performed on compounds **6c**,**d** **9c**, and **10b**, allowed us to assess the right conformation of nitrooxyalkyl ester and ether side chains of these molecules within the COX-2 active site.

dx.doi.org/10.1021/jm301370e | J. Med. Chem. 2013, 56, 3191−3206

EXPERIMENTAL SECTION

Chemistry. All chemicals used were of reagent grade. Yields refer to purified products and are not optimized. Melting points were determined in open capillaries on a Gallenkamp apparatus and are uncorrected. Merck silica gel 60 (230−400 mesh) was used for column chromatography. Merck TLC plates and silica gel 60 F_{254} were used for TLC. ^{1}H-NMR spectra were recorded with a Bruker AC 200 spectrometer in the indicated solvent (TMS as internal standard). The values of the chemical shifts are expressed in ppm, and the coupling constants (J) are expressed in Hz. Mass spectra were recorded on a VG 70-250S (EI, 70 eV), a Varian Saturn 3, or a ThermoFinningan LCQdeca spectrometer. High resolution accurate mass measurements were recorded by an LTQ-Orbitrap (Thermo Fisher) spectrometer in positive ESI (for details see Supporting Information). Purity of compounds **9a−d**, **10a−c**, **17a−d**, and **18a−c** was assessed by RP-HPLC and was found to be higher than 95%. A VWR_Hitachi L-2130 pump system equipped with a VWR_Hitachi L-2400. Merck LiChroCART 125-4 C18 column was used in the HPLC analysis with (method A) acetonitrile−water−methanol (50:20:30) or (method B) methanol−acetonitrile (20:80) as the mobile phase at a flow rate of 0.7 mL/min. UV detection was achieved at 210 nm.

General Procedure for the Preparation of 1,5-Diaryl-3-(2-hydroxyethyl)pyrroles (11c,d). A solution of the suitable ethyl acetate ester[24] (1.3 mmol) in dry THF (5 mL) was added dropwise to a stirred suspension of lithium aluminum hydride (2.8 mmol) in dry THF (20 mL). After the mixture was stirred for 20 min under nitrogen atmosphere, the excess of the reducing agent was decomposed by careful addition of H_2O (2 mL). The inorganic material was filtered off and washed with THF. The filtrate was dried (Na_2SO_4) and evaporated under reduced pressure. The residue, purified by flash chromatography (EtOAc/hexane, 6:4 v/v), gave the expected compound. Compounds **11a,b** were resynthesized starting from the suitable ester, and their spectroscopic and analytical data were consistent with those that were previously reported.[24] The same procedure was used for the preparation of novel compounds **11c,d**.

General Procedure for the Preparation of 1,5-Diaryl-2-methyl-3-(2-((tetrahydro-2*H*-2-yloxy)alkoxy)ethyl)-1*H*-pyrrole Derivatives (15a−d and 16a−c). Alcohols **11a−c**, or **11d** (2,7 mmol) and tetrabutyl ammonium bromide (1,35 mmol), cooled to 0 °C were treated with a solution of NaOH 50% p/p (100 mL) and the suitable 2-(bromoalkoxy)tetrahydro-2*H*-pyran derivative (10.84 mmol). After being stirred under a nitrogen atmosphere at 70 °C for 72 h, the mixture was treated with brine (5 mL) and water (20 mL). EtOAc was then added, and the organic extract was washed to neutrality with water and brine, dried over Na_2SO_4, filtered, and concentrated in vacuo. The crude residue, purified by flash chromatography, gave the expected compound.

General Procedure for the Preparation of (2-(1,5-Diaryl-2-methyl-1*H*-pyrrol-3-yl)alkoxy)alcohols (17a−d and 18a−c). To a solution of the suitable alcohol **15** or **16** (0.7 mmol) in MeOH (6 mL) pyridinium *p*-toluenesulfonate (PPTS) (0.1 mmol) was added. The mixture was then warmed at 55 °C for 1 h while being stirred. H_2O (30 mL) was added, and the mixture was extracted with diethyl ether (20 mL). The organic layers were washed with brine (20 mL) and H_2O (20 mL), dried over Na_2SO_4, and filtered. The residue, obtained after evaporation of the solvent, was purified by flash chromatography to give the expected compound.

2-(2-(1-(4-Fluorophenyl)-2-methyl-5-(4-(methylsulfonyl)-phenyl)-1*H*-pyrrol-3-yl)ethoxy)ethanol (17c). White solid. Yield 56%. Mp 110−114 °C. ^{1}H-NMR ($CDCl_3$) ppm: 2.01 (broad s, 1H); 2.03(s,3H); 2.76 (t,2H); 2.98 (s,3H); 3.57−3.71 (m,6H); 6.42 (s,1H); 7.02−7.14 (m,6H); 7.61−7.66 (m,2H). MS-ESI: m/z 439 ($M + Na^+$).

General Procedure for the Preparation of 2-(2-(1,5-Diaryl-2-methyl-1*H*-pyrrol-3-yl)ethoxy)alkyl Methanesulfonate Derivatives (19a−d and 20a−c). To a solution of the suitable alcohol **17a−d** or **18a−c** (0.3 mmol) dissolved into CH_2Cl_2 (10 mL) 4-(dimethylamino)pyridine (DMAP) (0.03 mmol) and *N*,*N*-diisopropylethylamine (DIPEA) (0.5 mmol) were added in sequence. The solution was cooled at 0 °C, and mesyl chloride (0.6 mmol) was added dropwise. After being stirred for 3 h at room temperature, the mixture was treated with H_2O (5 mL) and the organic layer washed to neutrality with saturated $NaHCO_3$ (5 mL) and H_2O (5 mL), dried, filtered, and evaporated to give the expected mesylate as an oil that was purified by flash chromatography.

General Procedure for the Preparation of Nitrooxy Derivatives (9a−d and 10a−c). A solution of the appropriate mesyl derivative **19a−d** or **20a−c** (0.3 mmol) in toluene (5 mL) was treated with tetrabutylammonium nitrate (0.9 mmol), and the mixture was stirred to reflux for 1 h. H_2O was added and the mixture extracted with EtOAc. The organic layer was then washed with brine and H_2O, dried over Na_2SO_4, filtered and the solvent evaporated in vacuo. The crude product was purified by flash chromatography on silica gel to give the expected compounds.

2-(2-(1-(4-Fluorophenyl)-2-methyl-5-(4-(methylsulfonyl)-phenyl)-1*H*-pyrrol-3-yl)ethoxy)ethyl Nitrate (9c). Orange needles from methanol (yield 70%). Mp 104−105 °C. ^{1}H-NMR ($CDCl_3$) δ (ppm): 2.03 (s, 3H); 2.75 (t, 2H); 2.98 (s, 3H); 3.63−3.78 (m, 4H); 4.62 (t, 2H); 6.43 (s, 1H); 7.03−7.16 (m, 6H); 7.63−7.67 (m, 2H). MS-ESI: m/z 485 ($M + Na^+$).

Pharmacology. In Vitro Anti-Inflammatory Study. The in vitro profiles of compounds **9a−d**, **10a−c**, **18a−d**, and **19a−c**, related to their inhibitory activity toward both COX-1 and COX-2 isoenzymes, were evaluated through a cell-based assay employing murine monocyte/macrophage J774 cell lines. The cell line was grown in DMEM supplemented with 2 mM glutamine, 25 mM HEPES, 100 units/mL penicillin, 100 μg/mL streptomycin, 10% fetal bovine serum (FBS), and 1.2% sodium pyruvate. Cells were plated in 24-well culture plates at a density of 2.5×10^5 cells/mL or in 60 mm diameter culture dishes (3×10^6 cells per 3 mL per dish) and allowed to adhere at 37 °C in 5% CO_2 for 2 h. Immediately before the experiments, the culture medium was replaced with fresh medium and cells were stimulated as previously described.[51] The evaluation of COX-1 inhibitory activity was achieved by pretreating cells with the test compounds (10 μM) for 15 min and then incubating them at 37 °C for 30 min with 15 μM arachidonic acid to activate the constitutive COX. For the compounds with COX-1 % inhibition higher than 50% (at 10 μM), the cells were also treated with lower concentrations (0.1−1 μM). At the end of the incubation, the supernatants were collected for the measurement of prostaglandin E_2 (PGE_2) levels by a radioimmunoassay (RIA). To evaluate COX-2 activity, the cells were stimulated for 24 h with *Escherichia coli* lipopolysaccharide (LPS, 10 μg/mL) to induce COX-2, both in the absence and in the presence of the test compounds (0.01−10 μM). Celecoxib was used as a reference compound for the selectivity index. The supernatants were collected for the measurement of PGE_2 by means of RIA.

Ex Vivo Vasorelaxing Activity. All the experimental procedures were carried out following the guidelines of the European Community Council Directive 86-609. The effects of the compounds were tested on isolated thoracic aortic rings of male normotensive Wistar rats (250−350 g), as previously described.[52] After a light ether anesthesia, rats were sacrificed by cervical dislocation and bleeding. The aortae were immediately excised, freed of extraneous tissues, and the endothelial layer was removed by gently rubbing the intimal surface of the vessels with a hypodermic needle. Five millimeter wide aortic rings were suspended, under a preload of 2 g, in 20 mL organ baths containing Tyrode solution (composition of saline in mM: NaCl 136.8; KCl 2.95; $CaCl_2$ 1.80; $MgSO_4$ 1.05; NaH_2PO_4 0.41; $NaHCO_3$ 11.9; glucose 5.5) thermostated at 37 °C and continuously gassed with a mixture of O_2 (95%) and CO_2 (5%). Changes in tension were recorded by means of an isometric transducer (Grass FTO3) connected with a computerized system (Biopac). After an equilibration period of 60 min, the endothelium removal was confirmed by the administration of acetylcholine (ACh) (10 μM) to KCl (30 mM) precontracted vascular rings. A relaxation of <10% of the KCl-induced contraction was considered representative of an acceptable lack of the endothelial layer, while the organs showing a relaxation of ≥10% (i.e., significant presence of the endothelium) were discarded. From 30 to 40 min after the confirmation of the endothelium removal, the aortic preparations were contracted by a single concentration of KCl (30 mM), and when the contraction reached a stable plateau, 3-fold

dx.doi.org/10.1021/jm301370e | J. Med. Chem. 2013, 56, 3191−3206

increasing concentrations of compounds (1nM to 10 μM) were added. Preliminary experiments showed that the KCl (30 mM) induced contractions remained in a stable tonic state for at least 40 min. The same experiments were also carried out in the presence of a well-known GC inhibitor: ODQ 1 μM, which was incubated in aortic preparations after the endothelium removal was confirmed. The vasorelaxing efficacy was evaluated as maximal vasorelaxing response (E_{max}), expressed as a percentage (%) of the contractile tone induced by KCl 30 mM. When the limit concentration of 10 μM (the highest concentration that could be administered) of the tested compounds did not reach the maximal effect, the parameter of efficacy represented the vasorelaxing response, expressed as a percentage (%) of the contractile tone induced by KCl 30 mM, evoked by this limit concentration. The parameter of potency was expressed as pIC_{50}, calculated as the negative logarithm of the molar concentration of the tested compounds evoking a half reduction of the contractile tone induced by KCl 30 mM. The pIC_{50} could not be calculated for those compounds showing an efficacy parameter lower than 50%. The parameters of efficacy and potency were expressed as the mean ± standard error for 6−10 experiments. Two-way ANOVA was selected as statistical analysis, and $P < 0.05$ was considered representative of significant statistical differences. The experimental data were analyzed by a computer fitting procedure (software: GraphPad Prism, version 4.0).

In Vitro Human Whole Blood (HWB) Assay. Compounds **9a** and **17c** were also evaluated for COX-1 versus COX-2 selectivity in a HWB assay. Three healthy volunteers (two females and one male, aged 29 ± 3 years) were enrolled to participate in the study after its approval by the Ethical Committee of the University of Chieti, Italy. Informed consent was obtained from each subject. Compounds **9a** (0.05−150 mM) and **17c** (0.05−150 mM) were dissolved in DMSO. Aliquots of the solutions (2 μL) or vehicle were pipetted directly into test tubes to give final concentrations of 0.1−300 μM in whole blood samples. To evaluate COX-2 activity, 1 mL aliquots of peripheral venous blood samples containing 10 IU of sodium heparin were incubated in the presence of LPS (10 μg/mL) or saline for 24 h at 37 °C, as previously described.[53] The contribution of platelet COX-1 was suppressed by pretreating the subjects with aspirin (300 mg, 48 h) before sampling. Plasma was separated by centrifugation (10 min at 2000 rpm) and kept at −80 °C until assayed for PGE_2 as an index of monocyte COX-2 activity. Moreover, peripheral venous blood samples were drawn from the same donors after they had not taken any NSAID for the 2 weeks preceding the study. Aliquots (1 mL) of whole blood were immediately transferred into glass tubes and allowed to clot at 37 °C for 1 h. Serum was separated by centrifugation (10 min at 3000 rpm) and kept at −80 °C until assayed for TXB_2. Whole blood TXB_2 production was measured as a reflection of maximal platelet COX-1 activity in response to endogenously formed thrombin.[54]

Analysis of PGE_2 and TXB_2. PGE_2 and TXB_2 concentrations were measured by previously described and validated radioimmunoassays.[53,54] Unextracted plasma and serum samples were diluted in the standard diluent of the assay (0.02 M phosphate buffer, pH 7.4) and assayed in a volume of 1.5 mL at a final dilution of 1:50 to 1:30000. [^{3}H]PGE_2 or [^{3}H]TXB_2 (3000 cpm, specific activity of >100 Ci/mmol, 1:100000 dilution) and anti-TXB_2 (1:120000 dilution) sera were used. The least detectable concentration was 1−2 pg/mL for both prostanoids.[53,54]

In Vivo Anti-Inflammatory and Antinociceptive Study. In vivo anti-inflammatory activity of the title compounds was also assessed and performed as follows.

Animals. Male Swiss albino mice (23−25g) and Sprague−Dawley or Wistar rats (150−200 g) were used. Fifteen mice and four rats were housed per cage. The cages were placed in the experimental room 24 h before the test for acclimatization. The animals were fed with a standard laboratory diet and tap water ad libitum and kept at 23 ± 1 °C with a 12 h light/dark cycle, light on at 7 a.m. All experiments were carried out in accordance with the NIH Guide for the Care and Use of Laboratory Animals. All efforts were made to minimize animal suffering and to reduce the number of animals used.

Paw-Pressure Test. The paw-pressure test was performed by inducing an inflammatory process by the intraplantar (ipl) carrageenan (0.1 mL, 1%) administration 4 h before the test The nociceptive threshold in the rat was determined with an analgesimeter, according to the method described by Leighton et al.[55] Threshold pressure was measured before and 30, 60, and 120 min after treatment. An arbitrary cutoff value of 250 g was adopted.

Carrageenan-Induced Edema. The carrageenan-induced paw edema test was also performed. Rat paw volumes were measured using a plethysmometer. Four hours after the injection of carrageenan (0.1 mL injection of 1.0%), the paw volume of the right hind paw was measured and compared with saline/carrageenan treated controls. Rats received test compounds 3 h 30 min after carrageenan. The results are reported as paw volume expressed in mL.

Antinociceptive Assay. Antinociceptive activity was determined by means of an intraperitoneal (ip) injection of a 0.6% acetic acid (10 mL/kg) induced writhing in the mouse abdominal constriction test according to Koster.[56] The number of stretching movements was counted for 10 min, starting 5 min after acetic acid injection.

Monosodium Iodoacetate Test. An amount of 2 mg of monosodium iodioacetate (MIA) was solubilized in a volume of 25 μL of saline and injected into the left knee joint of anesthetized rats. Control rats were treated with an equal volume of saline. Animals received a repeated administration (14 days twice daily) of **9c** or **17c** (20 mg kg^{-1} po). The administration of MIA induces in rats a hyperalgesic response to mechanical stimuli that reaches its statistical significance 5 days after administration and persists for 4 weeks. Test were performed 15−21 days after MIA injection.

Statistical Analysis. Triplicate wells were used for the various conditions of the treatment in the cell culture assay throughout the experiments. Results are expressed as the mean of three experiments of the % inhibition of PGE_2 production by test compounds with respect to control samples. Data fit was obtained using the sigmoidal dose−response equation (variable slope) (GraphPad software). The IC_{50} values were calculated with GraphPad Instat, and the data fit was obtained using the sigmoidal dose−response equation (variable slope) (GraphPad).

Results from paw-pressure and writhing tests are given as the mean (SEM, analysis of variance (ANOVA)), followed by Fisher's PLSD procedure for post hoc comparison, used to verify the significance between two means. P values lower than 0.05 were considered significant. The data were analyzed by the StatView for the Macintosh computer program.

Explant Cartilage Cultures. Slices were removed from the metacarpophalangeal joints of adult bovine animals (18−20 months old) obtained from the slaughterhouse. Joints were opened under aseptic conditions, and slices were cut from the exposed articular surface and washed with Dulbecco's modified Eagle medium (DMEM) containing 500 units/mL of penicillin−streptomycin. Slices were cut so that each slice was greater than 50 mg in weight. During the harvest, care was taken not to include cartilage dose to the junction with the synovium and the calcified cartilage. Slices, about 100 mg quantities, were then transferred to each well of 24-well tissue culture plates. The wells were filled with 1.5 mL of DMEM and incubated at 37 °C in 5% CO_2. The medium was changed at 1 day and 2 days in order to allow effusion of PG from the cut areas. Assays during this time showed a progressive decrease in PG (proteoglycan) release that plateaued on the third day. On the third day, DMEM test solutions were added to the explants. Culturing was done in nearly all cases with DMEM without serum in order not to contaminate the culture with Fn-containing serum or with protease inhibitors. In some experiments, where optimal cell growth was necessary, DMEM was supplemented with IGF-1 at a final concentration of 20 ng/mL. IGF in serum-free medium has been shown to promote PG synthesis as optimally as 20% fetal bovine serum.[34] Analysis of GAG release by 1,9-dimethylmethylene blue (DMB) assay was performed according to the colorimetric Farndale method.[35]

Computational Details. Inhibitor Setup. The structures of the inhibitors used in the docking simulations were generated by means of Extensible Computational Chemistry Environment (ECCE) soft-

ware[57] and then geometry-optimized by means of NWChem (100 steps of RHF, 6-31G*). Partial atomic charges RESP were calculated by means of the NWChem and then used in the following docking simulations.[58] All relevant torsion angles were treated as rotatable during the docking process, thus allowing a search for the conformational space.

Enzyme Setup. The COX-2 protein was set up for docking as follows: polar hydrogens were added by means of ECCE software, and Kollman united-atom partial charges were assigned.[59] The ADDSOL utility of AutoDock was used to add solvation parameters to the protein structures, and the grid maps representing the proteins in the docking process were calculated by means of AutoGrid. The grids, one for each atom type in the inhibitor plus one for the electrostatic interactions, were chosen to be large enough to include not only the cyclooxygenase sites but also a significant part of the protein around it. As a consequence, the dimensions of grid maps were 59 × 45 × 59 points with a grid point spacing of 0.375 Å for COX-2 for all docking calculations.

Docking Calculations. Compounds **6d** and **10b** were docked into the enzymes using AutoDock 4.2.[42] Docking simulations of the compounds were carried out using the Lamarckian genetic algorithm and through a protocol with an initial population of 300 randomly placed individuals, a maximum number of 25 million energy evaluations, a mutation rate of 0.02, a crossover rate of 0.80, and an elitism value of 1. The pseudo Solis and Wets algorithm with a maximum of 300 interactions was applied for the local search. Two-hundred independent docking runs were carried out for each inhibitor, and the resulting conformations that differed by less than 2.0 Å in positional root-mean-square deviation (rmsd) were clustered together. Cluster analysis was performed by selecting the most populated cluster, which in all cases agreed with the biological affinity data. All the relevant torsion angles were treated as rotatable during the docking process, thus allowing a search of the conformational space.

Enzyme Setup. The COX-2 protein was set up for docking as follows: polar hydrogens were added by means of ECCE software, and Kollman united-atom partial charges were assigned. The ADDSOL utility of AutoDock 4.2[42] was used to add solvation parameters to the protein structures, and the grid maps representing the proteins in the docking process were calculated using AutoGrid. The grids, one for each atom type in the inhibitor plus one for the electrostatic interactions, were chosen to be large enough to include not only the cyclooxygenase sites but also a significant part of the protein around it. As a consequence, the dimensions of grid maps were 59 × 45 × 59 points with a grid point spacing of 0.375 Å for COX-2 for all docking calculations.

Molecular Dynamics. According to Desmond guidelines (*Desmond User Manual*, version 3.0; Schrödinger, LLC: New York, NY, 2011), the representative poses belonging to the best clustered solutions of the complexes COX-2−**6d** and COX-2−**10b**, obtained by means of docking calculations, were imported into Schrödinger Maestro molecular modeling environment[60] and submitted to Protein Preparation Wizard workflow[61] in order to obtain reasonable complexes used as starting point for molecular dynamics (MD) simulation protocol. MD simulations were carried out by Desmond 3.0 package[62,63] using Maestro molecular modeling environment as graphical interface.[60] The above-mentioned complexes (COX-2−**6d** and COX-2−**10b**; Figures 3 and 4, respectively) were imported in Maestro and solvated into an orthorhombic box filled with water, simulated by TIP3P model.[64] OPLS_2005 force field[65,66] was applied for MD calculations. Na^+ and Cl^- ions were added to provide a final salt concentration of 0.15 M in order to simulate physiological concentration of monovalent ions. (*Desmond User Manual*, version 3.0; Schrödinger, LLC: New York, NY, 2011). Constant temperature (300 K) and pressure (1.013 25 bar) were employed with *NPT* (constant number of particles, pressure, and temperature) as ensemble class. RESPA integrator[67] was used in order to integrate the equations of motion, with an inner time step of 2.0 fs for bonded interactions and nonbonded interactions within the short-range cutoff. Nose−Hoover thermostats[68] were used to keep the constant simulation temperature, and the Martyna−Tobias−Klein method[69] was applied to control the pressure. Long-range electrostatic interactions were calculated by particle-mesh Ewald method (PME).[70] The cutoff for van der Waals and short-range electrostatic interactions was set at 9.0 Å. The equilibration of the system was performed with the default protocol provided in Desmond, which consists of a series of restrained minimizations and molecular dynamics simulations used to slowly relax the system. Consequently, a single trajectory for each complex of 5 ns was calculated.

■ ASSOCIATED CONTENT

Ⓢ Supporting Information

Experimental, physicochemical, elemental analysis results, and spectroscopic data of compounds along with single crystal X-ray structures of compounds **6c**, **9c**, and **17c**; analysis of GAG release by colorimetric Farndale's method and in vivo (blood and intestine) conversion of naproxcinod into naproxen and NOBA by esterases; ^{1}H- and ^{13}C-NMR studies performed on compounds **6c**,**d**, **9c**, and **10b**; high resolution accurate mass measurements. This material is available free of charge via the Internet at http://pubs.acs.org.

■ AUTHOR INFORMATION

Corresponding Author

*Phone: +39 577 234173. Fax: +39 577 234333. E-mail: maurizio.anzini@unisi.it

Author Contributions

The manuscript was written with the contributions of all the authors. All the authors have expressly approved the final version of the manuscript.

Notes

The authors declare no competing financial interest.

■ ACKNOWLEDGMENTS

We are grateful to Dr. Laura Salvini (Toscana Life Sciences, Siena, Italy) for the recording of high resolution mass spectra and to Dr. Francesco Berrettini (C.I.A.D.S., University of Siena, Italy) for X-ray diffraction studies. Prof. Stefania D'Agata D'Ottavi's careful reading of the manuscript is also acknowledged. We thank Rottapharm Madaus (Monza, Italy) for financial support of this research.

■ ABBREVIATIONS USED

tNSAID, traditional nonsteroidal anti-inflammatory drug; COXIB, cyclooxygenase-2 inhibitor; COX, cyclooxygenase; GI, gastrointestinal; NO, nitric oxide; iNOS, inducible nitric oxide synthase; cNOS, constitutive nitric oxide synthase; AA, arachidonic acid; GC, guanylate cyclase; c-GMP, cyclic guanosine monophosphate; CV, cardiovascular; CINOD, cyclooxygenase-inhibiting nitric oxide donors; EDC, 1-ethyl-3-(3-dimethylaminopropyl)carbodiimide; DMAP, dimethylaminopyridine; DIPEA, *N*,*N*′-diisopropylethylamine; Ach, acetylcholine; DMEM, Dulbecco's modified Eagle medium; PGE_2, prostaglandin E_2; FBS, fetal bovine serum; LPS, lipopolysaccharide; RIA, radioimmunoassay; TX, thromboxane; CMC, carboxymethylcellulose; ODQ, 1*H*-[1,2,4]oxadiazolo[4,3-*a*]-quinoxalin-1-one; ipl, intraplantar; po, per os; ip, intraperitoneal; NOBA, 4-(nitroxy)butanol; GTN, glyceryl trinitrate; E_{max}, maximal vasorelaxing response; MIA, monosodium iodoacetate; 1D NOE, one-dimensional nuclear Overhauser effect; 2D-NOE, two-dimensional nuclear Overhauser effect

REFERENCES

(1) Zhang, W.; Moskowitz, R. W.; Nuki, G.; Abramson, S.; Altman, R. D.; Arden, N.; Bierma-Zeinstra, S.; Brandt, K. D.; Croft, P.; Doherty, M.; Dougados, M.; Hochberg, M.; Hunter, D. J.; Kwoh, K.; Lohmander, L. S.; Tugwell, P. OARSI Recommendations for the Management of Hip and Knee Osteoarthritis, Part I: Critical Appraisal of Existing Treatment Guidelines and Systematic Review of Current Research Evidence. *Osteoarthritis Cartilage* **2007**, *15*, 981−1000.

(2) Davies, N. M.; Anderson, K. E. Clinical Pharmacokinetics of Diclofenac. Therapeutic Insights and Pitfalls. *Clin. Pharmacokinet.* **1997**, *33*, 184−213.

(3) Ricciotti, E.; FitzGerald, G. A. Prostaglandins and Inflammation. *Arterioscler., Thromb., Vasc. Biol.* **2011**, *31*, 986−1000.

(4) FitzgGerald, G. A.; Patrono, C. The Coxibs, Selective Inhibitors of Cyclooxygenase-2. *N. Engl. J. Med.* **2001**, *345*, 433−442.

(5) Lanas, A. A Review of the Gastrointestinal Safety Data: A Gastroenterologist's Perspective. *Rheumatology* **2010**, *49* (S2), 3−10.

(6) Antman, E. M.; DeMets, D.; Loscalzo, J. Cyclooxygenase Inhibition and Cardiovascular Risk. *Circulation* **2005**, *112*, 759−70.

(7) Di Francesco, L.; Totani, L.; Dovizio, M.; Piccoli, A.; Di Francesco, A.; Salvatore, T.; Pandolfi, A.; Evangelista, V.; Dercho, R. A.; Seta, F.; Patrignani, P. Induction of Prostacyclin by Steady Laminar Shear Stress Suppresses Tumor Necrosis Factor-alpha Biosynthesis via Heme Oxygenase-1 in Human Endothelial Cells. *Circ. Res.* **2009**, *104*, 506−513.

(8) Yu, Y.; Ricciotti, E.; Scalia, R.; Tang, S. Y.; Grant, G.; Yu, Z.; Landesberg, G.; Crichton, I.; Wu, W.; Puré, E.; Funk, C. D.; FitzGerald, G. A. Vascular COX-2 Modulates Blood Pressure and Thrombosis in Mice. *Sci. Transl. Med.* **2012**, *4*, 132ra54.

(9) Gewaltig, M. T.; Kojda, G. Vasoprotection by Nitric Oxide: Mechanisms and Therapeutic Potential. *Cardiovasc. Res.* **2002**, *55*, 250−260.

(10) Grosser, T.; Fries, S.; FitzGerald, G. A. Biological Basis for the Cardiovascular Consequences of COX-2 Inhibition: Therapeutic Challenges and Opportunities. *J. Clin. Invest.* **2006**, *116*, 4−15.

(11) Wallace, J. L.; Miller, M. J. Nitric Oxide in Mucosal Defence: A Little Goes a Long Way. *Gastroenterology* **2000**, *119*, 512−520.

(12) Whittle, J. R. Cicloxygenase and Nitric Oxide Systems in the Gut as Therapeutic Targets for Safer Anti-Inflammatory Drugs. *Curr. Opin. Pharmacol.* **2004**, *4*, 538−545.

(13) Muscará, M. N.; Wallace, J. L. COX-Inhibiting Nitric Oxide Donors (CINODs): Potential Benefits on Cardiovascular and Renal Function. *Cardiovasc. Hematol. Agents Med. Chem* **2006**, *4*, 155−164.

(14) Geusens, P. Naproxcinod, a New Cyclooxygenase-Inhibiting Nitric Oxide Donator (CINOD). *Expert Opin. Biol. Ther.* **2009**, *9*, 649−657.

(15) White, W. B.; Schnitzer, T. J.; Fleming, R.; Duquesroix, B.; Beekman, M. Effects of the Cyclooxygenase Inhibiting Nitric Oxide Donator Naproxcinod versus Naproxen on Systemic Blood Pressure in Patients with Osetoarthritis. *Am. J. Cardiol.* **2009**, *104*, 840−845.

(16) Weber, M. A. Treatment of Patients with Hypertension and Arthritis Pain: New Concepts. *Am. J. Med.* **2009**, *122*, S16−S22.

(17) Govoni, M.; Casagrande, S.; Maucci, R.; Chiroli, V.; Tocchetti, P. In Vitro Metabolism of (Nitroxy)butyl Ester Nitric Oxide-Releasing Compounds: Comparison with Glyceryl Trinitrate. *J. Pharmacol. Exp. Ther.* **2006**, *317*, 752−776.

(18) Berndt, G.; Grosser, N.; Hoogstraate, J.; Schröder, H. A Common Pathway of Nitric Oxide Release from AZD3582 and Glyceryl Trinitrate. *Eur. J. Pharm. Sci.* **2004**, *21*, 331−335.

(19) Capone, M. L.; Tacconelli, S.; Sciulli, M. G.; Anzellotti, P.; Di Francesco, L.; Merciaro, G.; Di Gregorio, P.; Patrignani, P. Human Pharmacology of Naproxen Sodium. *J. Pharmacol. Exp. Ther.* **2007**, *322*, 453−460.

(20) Cappelli, A.; Anzini, M.; Biava, M.; Makovec, F.; Giordani, A.; Caselli, G.; Rovati, L. C. 3-Substituted-1,5-Diaryl-2-alkyl-pyrroles Highly Selective and Orally Effective COX-2 Inhibitors. PCT Int. Appl. WO2008014821, 2008.

(21) Anzini, M.; Rovini, M.; Cappelli, A.; Vomero, S.; Manetti, F.; Botta, M.; Sautebin, L.; Rossi, A.; Ghelardini, C.; Norcini, M.; Giordani, A.; Makovec, F.; Anzellotti, P.; Patrignani, P.; Biava, M. Synthesis, Biological Evaluation, and Enzyme Docking Simulations of 1,5-Diarylpyrrole-3-alkoxyethyl Ethers as Highly Selective COX-2 Inhibitors Endowed with Anti-Inflammatory and Antinociceptive Activity. *J. Med. Chem.* **2008**, *51*, 4476−4481.

(22) Biava, M.; Porretta, G. C.; Poce, G.; Battilocchio, C.; Manetti, F.; Botta, M.; Forli, S.; Sautebin, L.; Rossi, A.; Pergola, C.; Ghelardini, C.; Galeotti, N.; Makovec, F.; Giordani, A.; Anzellotti, P.; Patrignani, P.; Anzini, M. Novel Ester and Acid Derivatives of the 1,5-Diarylpyrrole Scaffold as Anti-Inflammatory and Analgesic Agents. Synthesis and in Vitro and in Vivo Biological Evaluation. *J. Med. Chem.* **2010**, *53*, 723−733 and references cited therein.

(23) Giordani, A.; Biava, M.; Anzini, M.; Calderone, V.; Rovati, L. 1,5-Diaryl-2-alkyl-pyrrole-3-Substituted Nitro Esters Selective COX-2 Inhibitors and Nitric Oxide Donors. WO2012032479 A1, 2012.

(24) Biava, M.; Porretta, G. C.; Poce, G.; Battilocchio, C.; Salvatore Alfonso, S.; Rovini, M.; Valenti, S.; Giorgi, G.; Calderone, V.; Martelli, A.; Testai, L.; Sautebin, L.; Rossi, A.; Papa, G.; Ghelardini, C.; Di Cesare Mannelli, L.; Giordani, A.; Anzellotti, P.; Patrignani, P.; Anzini, M. Novel Analgesic/Anti-Inflammatory Agents: Diarylpyrrole Acetic Esters Endowed with Nitric Oxide Releasing Properties. *J. Med. Chem.* **2011**, *54*, 7759−7771.

(25) Martelli, A.; Breschi, M. C.; Calderone, V. Pharmacodynamic Hybrids Coupling Established Mechanisms of Action with Additional Nitric Oxide Releasing Properties. *Curr. Pharm. Des.* **2009**, *15*, 614−636.

(26) Pomonis, J. D.; Boulet, J. M.; Gottshall, S. L.; Phillips, S.; Sellers, R.; Bunton, T.; Walker, K. Development and Pharmacological Characterization of a Rat Model of Osteoarthritis Pain. *Pain* **2005**, *114*, 339−346.

(27) Kobayashi, K.; Imaizumi, R.; Sumichika, H.; Tanaka, H.; Goda, M.; Fukunari, A.; Komatsu, H. Sodium Iodoacetate-Induced Experimental Osteoarthritis and Associated Pain Model in Rats. *J. Vet. Med. Sci.* **2003**, *65*, 1195−1199.

(28) Pfernihough, J.; Gentry, C.; Malcangio, M.; Fox, A.; Rediske, J.; Pellas, T.; Kidd, B.; Bevan, S.; Winter, J. Pain Related Behaviour in Two Models of Osteoarthritis in the Rat Knee. *Pain* **2004**, *112*, 83−93.

(29) Guingamp, C.; Gegout-Pottie, P.; Philippe, L.; Terlain, B.; Netter, P.; Gillet, P. Mono-Iodoacetate-Induced Experimental Osteoarthritis. A Dose-Response Study of Loss of Mobility, Morphology, and Biochemistry. *Arthritis Rheum.* **1997**, *40*, 1670−1679.

(30) Janusz, M. J.; Hookfin, E. B.; Heitmeyer, S. A.; Woessner, J. F.; Freemont, A. J.; Hoyland, J. A.; Brown, K. K.; Hsieh, L. C.; Almstead, N. G.; De, B.; Natchus, M. G.; Pikul, S.; Taiwo, Y. O. Moderation of Iodoacetate-Induced Experimental Osteoarthritis in Rats by Matrix Metalloproteinase Inhibitors. *Osteoarthritis Cartilage* **2001**, *9*, 751−760.

(31) Wey, S.; Augustyniak, M. E.; Cochran, E. D.; Ellis, J. L.; Fang, X.; Garvey, D. S.; Janero, D. R.; Letts, L. G.; Martino, A. M.; Melim, T. L.; Murty, M. G.; Richardson, S. K.; Schroeder, J. D.; Selig, W. M.; Trocha, A. M.; Wexler, R. S.; Young, D. V.; Zemtseva, I. S.; Zifcak, B. M. Structure-Based Design, Synthesis, and Biological Evaluation of Indomethacin Derivatives as Cyclooxygenase-2 Inhibiting Nitric Oxide Donors. *J. Med. Chem.* **2007**, *50*, 6367−6382.

(32) Chan, P. S.; Caron, D. V. M; Rosa, G. J. M.; Orth, M. W. Glucosamine and Chondroitin Sulfate Regulate Gene Expression and Synthesis of Nitric Oxide and Prostaglandin E_2 in Articular Cartilage Explants. *Osteoarthritis Cartilage* **2005**, *13*, 387−394.

(33) Mort, J. S.; Roughley, P. J. Measurament of Glycosaminoglycan Release from Cartilage Explants. *Methods Med.* **2007**, *135*, 201−209.

(34) Homandberg, G. A.; Meyers, R.; Xie, D. I. Fibronectin Fragments Cause Chondrolysis of Bovine Articular Cartilage Slices in Culture. *J. Biol. Chem.* **1992**, *25*, 3597−3604.

(35) Farndale, R. W.; Buttle, D. J.; Barret, A. J. Improved Quantitation and Discrimination of Sulphated Glycosaminoglycans by Use of Dimethylmethylene Blue. *Biochim. Biophys. Acta* **1986**, *883*, 173−177.

(36) Patrignani, P.; Muramatsu, M.; Tanaka, M.; Fujita, A.; Otomo, S.; Aihara, H. Time-Dependent Inhibition of Prostaglandins Synthesis

by Nonsteroidal Antiinflammatory Drugs; Time-Dependent Alteration of Inhibitory Effect and Characteristics of its Active Site. *Jpn J. Pharmacol.* **1984**, *35*, 37−46.
(37) Huntjens, D. R; Danhof, M.; Della Pasqua, O. E. Pharmacokinetic−Pharmacodynamic Correlations and Biomarkers in the Development of COX-2 Inhibitors. *Rheumatology (Oxford, U. K.)* **2005**, *44*, 846−859.
(38) Baerwald, C.; Verdecchia, P.; Duquesroix, B.; Frayssinet, H.; Ferreira, T. Efficacy, Safety, and Effects on Blood Pressure of Naproxcinod 750 mg Twice Daily Compared with Placebo and Naproxen 500 mg Twice Daily in Patients with Osteoarthritis of the Hip: A Randomized, Double-Blind, Parallel-Group, Multicenter Study. *Arthritis Rheum.* **2010**, *62* (12), 3635−3644.
(39) Abramson, S. B. Nitric Oxide in Inflammation and Pain Associated with Osteoarthritis. *Arthritis Res. Ther.* **2008**, *10* (Suppl. 2), S2.
(40) Krebs, S. A Review on the Derivation of the Spin-Restricted Hartree−Fock (RHF) Self-Consistent Field (SCF) Equations for Open-Shell Systems. Description of Different Methods to Handle the Off-Diagonal Lagrangian Multipliers Coupling Closed and Open Shells. *Comput. Phys. Commun.* **1999**, *116*, 137−277.
(41) Yuanpeng, J. H.; Tejero, R.; Powers, R.; Montelione, G. T. A Topology-Constrained Distance Network Algorithm for Protein Structure Determination from NOESY Data. *Proteins* **2006**, *62*, 587−603.
(42) Morris, G. M.; Huey, R.; Lindstrom, W.; Sanner, M. F.; Belew, R. K.; Goodsell, D. S.; Olson, A. J. Autodock4 and AutoDockTools4: Automated Docking with Selective Receptor Flexiblity. *J. Comput. Chem.* **2009**, *16*, 2785−2791.
(43) Werlhi, F. W. In *Topics in Carbon-13 NMR Spectroscopy*; Levy, G. C., Ed.; Wiley: New York, 1976; Vol. 2, p 343.
(44) Lyerla, J. R., Jr.; Levy, G. C. In *Topics in Carbon-13 NMR Spectroscopy*; Levy, G. C.; Wiley: New York, 1974; Vol. *1*, p 74.
(45) Allerhand, A.; Doddrell, D.; Komoroski, R. Natural Abundance Carbon-13 Partially Relaxed Fourier Transform Nuclear Magnetic Resonance Spectra of Complex Molecules. *J. Chem. Phys.* **1971**, *55*, 189−198.
(46) Werlhi, F. W.; Wirthlin, T. *Interpretation of Carbon-13 NMR Spectra*; Heyden: London, 1980.
(47) Frey, M. N.; Koetzle, T. F.; Lehmann, M. S.; Hamilton, W. C. Precision Neutron Diffraction Structure Determination of Protein and Nucleic Acid Components. X. A Comparison Between the Crystal and Molecular Structures of L-Tyrosine and L-Tyrosine Hydrochloride. *J. Chem. Phys.* **1973**, *58*, 2547−2556.
(48) Noggle, J. H.; Shirmer, R. E. *The Nuclear Overhauser Effect*; Academic Press: New York, 1971.
(49) Neuhaus, D.; Williamson, M. *The Nuclear Overhauser Effect in Structural and Conformational Analysis*; VCH Publishers, Inc.: New York, 1989.
(50) Valensin, G.; Pogliani, L.; Ghelardoni, M.; Pestellini, V.; Sega, A. Nuclear Magnetic Resonance Study of Conformation and Dynamics in Solution of *p*-(*o*-Propyloxybenzamido)benzoate Diethyl(2-hydroxyethyl)methylammonium Bromide: A Smooth Muscle Relaxant Agent. *Can. J. Chem.* **1984**, *62*, 2131−2135.
(51) Rossi, A.; Ligresti, A.; Longo, R.; Russo, A.; Borrelli, F.; Sautebin, L. The Inhibitory Effect of Propolis and Caffeic Acid Phenethyl Ester on Cyclooxygenase Activity in J774 Macrophages. *Phytomedicine* **2002**, *9*, 530−535.
(52) Breschi, M. C.; Calderone, V.; Digiacomo, M.; Martelli, A.; Martinotti, E.; Minutolo, F.; Rapposelli, S.; Balsamo, A. NO-Sartans: A New Class of Pharmacodynamic Hybrids as Cardiovascular Drugs. *J. Med. Chem.* **2004**, *47*, 5597−5600.
(53) Patrignani, P.; Panara, M. R.; Greco, A.; Fusco, O.; Natoli, C.; Iacobelli, S.; Cipollone, F.; Ganci, A.; Creminon, C.; Maclouf, J.; Patrono, C. Biochemical and Pharmacological Characterization of the Cyclooxygenase Activity of Human Blood Prostaglandin Endoperoxide Synthases. *J. Pharmacol. Exp. Ther.* **1994**, *271*, 1705−1712.
(54) Patrono, C.; Ciabattoni, G.; Pinca, E.; Pugliese, F.; Castrucci, G.; De Salvo, A.; Satta, M. A.; Peskar, B. A. Low Dose Aspirin and Inhibition of Thromboxane B2 Production in Healthy Subjects. *Thromb. Res.* **1980**, *17*, 317−327.
(55) Leighton, G. E.; Rodriguez, R. E.; Hill, R. G.; Hughes, J. κ-Opioid Agonists Produce Antinociception after iv and icv but Not Intrathecal Administration in the Rat. *Br. J. Pharmacol.* **1988**, *93*, 553−560.
(56) Koster, R.; Anderson, M.; de Beer, E. J. Acetic Acid for Analgesic Screening. *Fed. Proc.* **1959**, *18*, 412−418.
(57) Black, G. D.; Schuchardt, K. L.; Gracio, D. K.; Palmer, B. The Extensible Computational Chemistry Environment: A Problem Solving Environment for High Performance Theoretical Chemistry. *Computational Science—ICCS 2003*, Proceedings 2660 of the International Conference Saint Petersburg Russian Federation, Melbourne, Australia; Sloot, P. M. A., Abramson, D., Bogdanov, A. V., Dongarra, J., Eds.; Springer Verlag: Berlin, 2003; Vol. *81*, pp 122−131.
(58) Valiev, M.; Bylaska, E. J.; Govind, N.; Kowalski, K.; Straatsma, T. P.; van Dam, H. J. J.; Wang, D.; Nieplocha, J.; Apra, E.; Windus, T. L.; de Jong, W. A. NWChem: A Comprehensive and Scalable Open-Source Solution for Large Scale Molecular Simulations. *Comput. Phys. Commun.* **2010**, *181*, 1477−1489.
(59) Khandelwal, A.; Lukacova, V.; Comez, D.; Kroll, D. M.; Raha, S.; Balaz, S. A. Combination of Docking, QM/MM Methods, and MD Simulation for Binding Affinity Estimation. *J. Med. Chem.* **2005**, *48*, 5437−5447.
(60) *Maestro*, version 9.2; Schrödinger, LLC: New York, NY, 2011.
(61) Schrodinger. Docs & Known Issues. Protein Preparation Wizard 2011. http://www.schrodinger.com/supportdocs/18/16.
(62) *Desmond Molecular Dynamics System*, version 3.0; Shaw Research: New York, NY, 2011. *Maestro-Desmond Interoperability Tools*, version 3.0; Schrodinger: New York, NY, 2011.
(63) Bowers, K. J.; Chow, E.; Xu, H.; Dror, R. O.; Eastwood, M. P.; Gregersen, B. A.; Klepeis, J. L.; Kolossvary, I.; Moraes, M. A.; Sacerdoti, F. D.; Salmon, J. K.; Shan, Y.; Shaw, D. E. Scalable Algorithms for Molecular Dynamics Simulations on Commodity Clusters. *SC '06*, Proceedings of the 2006 ACM/IEEE Conference on Supercomputing, New York, U.S., 2006; IEEE: Piscataway, NJ, 2006.
(64) Jorgensen, W. L.; Chandrasekhar, J.; Madura, J. D.; Impey, R. W.; Klein, M. L. Comparison of Simple Potential Function for Simulating Liquid Water. *J. Chem. Phys.* **1983**, *79*, 926−935.
(65) Jorgensen, W. L.; Maxwell, D. S.; Tirado-Rives, J. Development and Testing of the OPLS All Atom Force Field on Conformational Energetics and Properties of Organic Liquids. *J. Am. Chem. Soc.* **1996**, *118*, 11225−11236.
(66) Kaminski, G. A.; Friesner, R. A.; Tirado-Rives, J.; Jorgensen, W. L. Evaluation and Reparametrization of the OPLS-AA Force Field for Proteins via Comparison with Accurate Quantum Chemical Calculations on Peptides. *J. Phys. Chem. B* **2001**, *105*, 6474−6487.
(67) Humphreys, D. D.; Friesner, R. A.; Berne, B. J. A Multiple-Time-Step Molecular-Dynamics Algorithm for Macromolecules. *J. Phys. Chem.* **1994**, *98*, 6885−6892.
(68) Hoover, W. G. Canonical Dynamics—Equilibrium Phase-Space Distributions. *Phys. Rev. A* **1985**, *31*, 1695−1697.
(69) Martyna, G. J.; Tobias, D. J.; Klein, M. L. Constant-Pressure Molecular-Dynamics Algorithms. *J. Chem. Phys.* **1994**, *101*, 4177−4189.
(70) Essmann, U.; Perera, L.; Berkowitz, M. L.; Darden, T.; Lee, H.; Pedersen, L. G. A Smooth Particle Mesh Ewald Method. *J. Chem. Phys.* **1995**, *103*, 8577−8593.